AFWL-TR-88-29

AFWL-TR-
88-29

EVALUATION OF DATA ERRORS INTRODUCED BY NOISE, SAMPLING RATES AND COMPOSITE WAVEFORMS

Dean I. Lawry
Clayborne D. Taylor

November 1988

Final Report

AIR FORCE WEAPONS LABORATORY
Air Force Systems Command
Kirtland Air Force Base, NM 87117-6008

This final report was prepared by the Air Force Weapons Laboratory, Kirtland Air Force Base, New Mexico under Job Order 37630151. Mr Dean I. Lawry (NTA) was the Laboratory Project Officer-in-Charge.

When Government drawings, specifications, or other data are used for any purpose other than in connection with a definitely Government-related procurement, the United States Government incurs no responsibility or any obligation whatsoever. The fact that the Government may have formulated or in any way supplied the said drawings, specifications, or other data, is not to be regarded by implication, or otherwise in any manner construed, as licensing the holder, or any other person or corporation; or as conveying any rights or permission to manufacture, use, or sell any patented invention that may in any way be related thereto.

This report has been authored by employees of the United States Government. Accordingly, the United States Government retains a nonexclusive, royalty-free license to publish or otherwise reproduce the material contained herein, or allow others to do so, for United States Governmen' ourposes.

This report has been reviewed by the Public Affairs Off and is releasable to the National Technical Information Service (NT At NTIS, it will be available to the general public, including foreig tions.

If your address has changed, if you wish to be removed n our mailing list, or if your organization no longer employs the addresse. olease notify AFWL/NTA, Kirtland AFB, NM 87117-6008 to help us maintain a rrent mailing list.

This technical report has been reviewed and is approved - publication.

Dean I. Lawry

DEAN I. LAWRY
Project Officer

FOR THE COMMANDER

Harold T. Bishop

HAROLD T. BISHOP
Major, USAF
Chief, Applications Branch

FREDERICK M. JONAS
Lt Col, USAF
Chief, Aircraft and Missiles Div

DO NOT RETURN COPIES OF THIS REPORT UNLESS CONTRACTUAL OBLIGATIONS OR NOTICE ON A SPECIFIC DOCUMENT REQUIRES THAT IT BE RETURNED.

REPORT DOCUMENTATION PAGE

1a REPORT SECURITY CLASSIFICATION Unclassified	1b. RESTRICTIVE MARKINGS
2a SECURITY CLASSIFICATION AUTHORITY	3 DISTRIBUTION / AVAILABILITY OF REPORT Approved for public release; distribution unlimited.
2b DECLASSIFICATION DOWNGRADING SCHEDULE	
4 PERFORMING ORGANIZATION REPORT NUMBER(S) AFWL-TR-88-29	5. MONITORING ORGANIZATION REPORT NUMBER(S)
6a NAME OF PERFORMING ORGANIZATION Air Force Weapons Laboratory 6b OFFICE SYMBOL (If applicable) NTAA	7a NAME OF MONITORING ORGANIZATION
6c. ADDRESS (City, State, and ZIP Code) Kirtland Air Force Base, NM 87117-6008	7b ADDRESS (City, State, and ZIP Code)
8a. NAME OF FUNDING / SPONSORING ORGANIZATION 8b OFFICE SYMBOL (If applicable)	9 PROCUREMENT INSTRUMENT IDENTIFICATION NUMBER
8c. ADDRESS (City, State, and ZIP Code)	10 SOURCE OF FUNDING NUMBERS

PROGRAM ELEMENT NO	PROJECT NO	TASK NO	WORK UNIT ACCESSION NO
64711F	3763	01	51

11 TITLE (Include Security Classification)
EVALUATION OF DATA ERRORS INTRODUCED BY NOISE, SAMPLING RATES AND COMPOSITE WAVEFORMS

12 PERSONAL AUTHOR(S)
Lawry, Dean I.; Taylor, Clayborne D.

13a TYPE OF REPORT	13b TIME COVERED	14 DATE OF REPORT (Year, Month, Day)	15 PAGE COUNT
Final	FROM Jan 86 TO Oct 86	1988 November	60

16 SUPPLEMENTARY NOTATION

17 COSATI CODES			18 SUBJECT TERMS (Continue on reverse if necessary and identify by block number)
FIELD	GROUP	SUB-GROUP	EMP, Test, Data Processing, Errors, Noise, Sampling Rates, Data Trends, Aliasing,
20	15		

19 ABSTRACT (Continue on reverse if necessary and identify by block number)

The limitations of automatic data processing of transient signals are studied. Errors resulting from noise, sampling, and forming composite records are evaluated by considering analytical waveforms. The applications of digital filtering and trend removal are also considered.

Various norms of time-domain signals are computed with the resulting errors identified for certain waveforms generic to nuclear electromagnetic pulse (NEMP) test data.

20 DISTRIBUTION / AVAILABILITY OF ABSTRACT	21 ABSTRACT SECURITY CLASSIFICATION
☐ UNCLASSIFIED/UNLIMITED ☐ SAME AS RPT ☑ DTIC USERS	Unclassified
22a NAME OF RESPONSIBLE INDIVIDUAL Mr. Dean I. Lawry	22b TELEPHONE (Include Area Code) (505) 844-9791 22c OFFICE SYMBOL NTAA

DD FORM 1473, 84 MAR 83 APR edition may be used until exhausted
All other editions are obsolete.

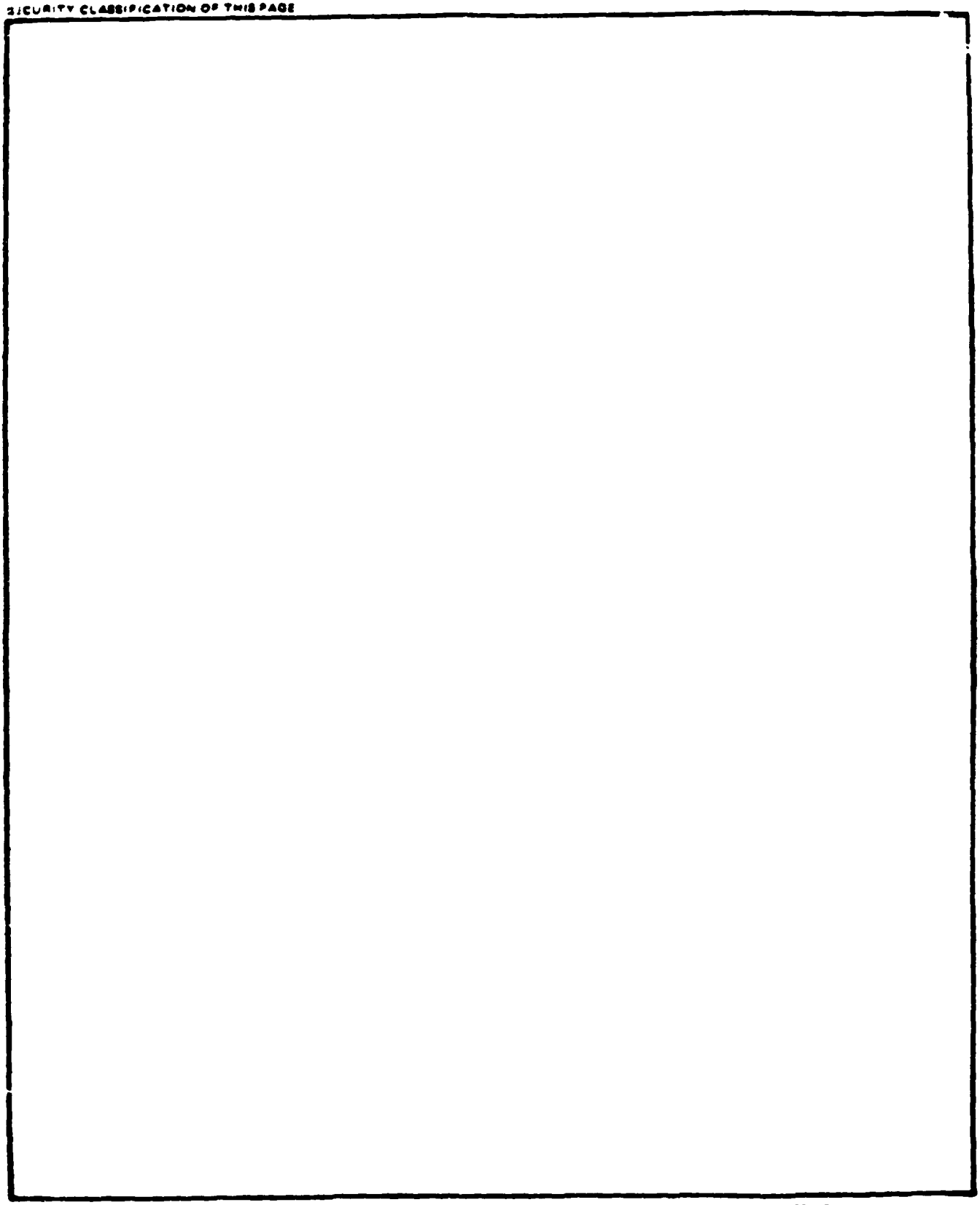

CONTENTS

1.0 INTRODUCTION

In obtaining recordings of fast transient signals, such as occur in nuclear electromagnetic pulse (NEMP) testing, the data system is configured typically as shown in Fig. 1. Because of the bandwidth and high-frequency spectral content, the handling of the data provides unique problems for the analyst. Typical error sources include:

Limited accuracy of the digitizer word

Extraneous electrical noise from the environmental excitation of the instrumentation system

Internal noise of the data system

Offset errors in the sampling device

Distortion from the nonlinearities of the data system

Excessive noise level resulting from the dynamic range limitation and low signal levels

Gain errors in the sampling device

Aperture errors in the sampling device

Monotonicity errors

Jitter in the digitizer

Dropout in the digitizer

Operator errors

Aliasing errors

Quantitatively, characterizing the cumulative effects of all of the noise sources is necessary in order to have complete confidence in the results. There are techniques for quantitating the random noise level in data (Ref. 1). However, it is virtually impossible to obtain even reasonable estimates for some of the noise sources. Aliasing noise is one of those.

The phenomenon of aliasing occurs when the sampled signal is not band limited or when it is undersampled; i.e., the sampling rate is below the Nyquist rate for a band-limited signal, where the Nyquist rate, S_N, is defined as

$$S_N = 2*f_{max} \quad (1)$$

Here f_{max} is the highest frequency of a band-limited signal. Consequently, aliasing occurs whenever the sampling rate, S, is below the Nyquist rate; i.e.,

$$S_N = \frac{1}{T} < S_N \quad (2)$$

where T is the sampling interval.

It is readily shown that a finite duration signal is not band limited and also that representing a transient by a finite length digitized record will always have aliasing error. Specifically, aliasing is the effect of a high frequency component in a signal taking on the indentity of a lower frequency component.

Generally, an aliasing error is not significant if the frequency content of the digitized signal is small for frequencies near and above the sampling rate. Undersampling is significant when it is manifested in the time domain by a signal variation that is too rapid for the sampling rate to capture it. It can be detected at times by an apparent clipping of signal peaks. In the frequency domain, the aliasing error is manifested by anomalous high frequencies near the Nyquist folding frequency (F_N).

$$F_N = \frac{1}{2} S \quad (3)$$

The effects of aliasing are exacerbated by the presence of wide band noise, especially random noise. However, aliasing effects can be minimized by filtering the data with a low pass filter having a cutoff frequency equal to the Nyquist folding frequency prior to digitizing. This may not be desirable since the filter itself will affect the frequency content below F_N and may disguise the presence of an important high frequency content.

In order to examine the cumulative effects of random noise, aliasing, and digital filtering, several NEMP-like signals (analytic representations) are considered. By successively adding noise and varying sampling rates, it is

possible to establish general behavior resulting from these effects and to quantify the results. Digital filtering is also introduced and general techniques for trend removal are discussed.

When broadband frequency signals are sampled at a rate fast enough to capture the high-frequency content, the limitation on the number of samples generally does not provide a sufficient record length to capture the low-frequency content of the signal. Consequently, multiple digitizers are used with sequenced triggering and different sampling rates. Typically, for NEMP test data, digitizers based on cathod-ray tube (CRT) scan converter technology are used where each unit obtains only 512 time samples. These records are combined to form a composite waveform. A uniformly sampled record is constructed via decimation and interpolation. Generally, the errors resulting from this procedure are not known. This topic is reserved for future study.

In order to categorize the characteristics of NEMP-induced signals that are important in invoking system responses, certain norms have been proposed (Ref. 2). The effects of sampling rates, random noise, digital filtering, and data trends on the norms are studied by using the analytical representations of typical data and introducing simulated noise and data trends. Results are obtained for various sampling rates and digital filtering schemes.

2.0 ANALYSIS

Several problems arise in collecting digitized response data from NEMP tests. Each of these problems are studied beginning with sampling.

2.1 SAMPLING

Typically, the voltage and current transients that result from NEMP excitation have substantial frequency content over the frequency range from 500 kHz to 100 MHz. Thus, the sampling of the data must faithfully capture that information. This introduces constraints on the sampling rate and the record length.

The upper bound on the frequency range of sampled data is determined by aliasing. A detailed explanation of aliasing is given by R. K. Otnes and L. Enochson in Ref. 3. It is not possible to determine precisely the least upper frequency bound. However, it is less than the Nyquist folding frequency given by Eq. 1. Ideally, the frequency content near the Nyquist frequency should be substantially below the peak frequency. If the frequency peaks near the Nyquist folding frequency, then the spectrum of the digitized data will be contaminated by aliasing for frequencies substantially below the Nyquist folding frequency.

The lower bound on the frequency range of the digitized data depends upon the record length and the total time duration of the sampling. A fundamental computational concept is that of an effective resolution bandwidth (B_e), which is defined as

$$B_e = \frac{1}{NT} \tag{4}$$

where N is the number of time samples accumulated during a given signal time interval, T. Any variations in the spectrum of the signal being digitized that occur over a bandwidth less than B_e will be substantially distorted by the digitizing. Consequently, the spectrum of the digitized signal will not be accurate for frequencies below f_L where

$$f_L \approx B_e \tag{5}$$

Moreover, it should be noted that resonant peaks that are narrower than B_e will not be correctly preserved in the digitized signal.

In general, the instrumentation (sensors, data link, etc.) limits the frequency band of accurate data. Typically, the upper limit on frequency for NEMP testing is about 100 MHz. Therefore, a sampling rate of 200 x 10^6/s (or a sampling interval of 2 ns) is sufficient, providing that the spectral content is negligible above 100 MHz so that aliasing does not corrupt the spectrum below 100 MHz. One means of reducing this corruption is to use a low-pass filter. This is discussed in the next section.

2.2 DIGITAL FILTERING

Recent advances in digital filter development have made available a variety of filters that can be applied directly to digitized time-domain data. For example, filtering can be used to limit the bandwidth of the data and to interpolate between sampling points to eliminate dropout errors. However, care must be exercised in using digital filters since they can increase the noise level, introduce distortion, and become unstable in some applications.

Digital filtering may be used to reduce the aliasing in data, but requires a multistep process. First, the data are oversampled; i.e., they are sampled at a higher rate than is needed. Second, the data are then passed through a low-pass digital filter with the cutoff frequency equal to the Nyquist folding frequency for the sampling rate desired. Third, the filtered data are decimated to achieve the desired samoling rate. Of course, an alternative procedure could utilize a hard-wired low-pass filter and direct sampling at the desired rate.

Choosing a digital filter involves consideration of the memory required, computational speed, accuracy, distortion and stability. there is no perfect rule to follow. However, cascading lower-order filters should be used rather than higher-order filters. This generally results in a filter that is more stable and freer of noise and distortion. But the cascade implementation is computationally less efficient than the combined higher-order filter.

If the response signal is smooth, then the spectral density at the lower frequencies must exceed the spectral density in the high frequency regime. Generally, this does occur for NEMP test data. In fact, it is often this property of the data that is used to determine the quality of the data. Since the spectrum of random noise is flat, the response signal spectrum becomes noise dominated at higher frequencies. By passing the data through a low-pass filter whose cutoff frequency equals the signal/noise crossover frequency, it is possible to reduce the noise and improve the signal-to-noise ratio (SNR). This crossover frequency often can be obtained by visually inspecting the Fourier transform of the measured data (for example, see Fig. 2).

Recently a technique was developed to automatically determine the signal/noise crossover frequency and apply an ideal low pass filter to improve the SNR (Ref. 4). As a result of this process, the response signal is approximated by a band-limited signal. Ther the discrete frequency Fourier transform pair is directly relatable to the continuous Fourier transform pair without approximations.

2.3 NOISE

There are a number of noise sources contributing to NEMP data. Many of these sources can be controlled by good measurement techniques. First, noise is picked up from the environment by the measurement instrumentation responding to the NEMP. Second, there is the inherent noise of the measurement system. Third, there is noise from the sampling device. Obviously, these noise sources do not produce totally random noise. However, for most practical purposes, the noise can be considered to be random.

2.4 DATA TRENDS

Slowly varying trends in NEMP data are common. These normally arise from integrated data where an error in the zero baseline when integrated produces a ramp function. Another source of data trends is the amplification of low frequency noise by an integrator. This type of trend is manifested in a slowly varying random behavior, and is somewhat dependent upon the sampling rate. The varying trend is best removed by a high-pass filter with the cutoff frequency set equal to f_L.

The ramp trend is easily recognized to be spurious. It is an example of a polynomial trend and can be removed by using least squares techniques (Ref. 3). If it is only required to remove the direct current (dc) bias and the ramp trends, then Eq. 6 is used.

$$\hat{x}(n) = x(n) - [C_o + (nT)C_1] \qquad n = 0,1,\ldots N-1 \tag{6}$$

where $\hat{x}(n)$ is the detrended data, $x(n)$ is the raw data and

$$C_o = [2(2N-1)\sum_{n=0}^{N-1} x(n) - 6\sum_{n=0}^{N-1} nx(n)]/N(N+1) \tag{7}$$

$$C_1 = 12\left[\sum_{n=0}^{N-1} nx(n) - 0.5(N-1)\sum_{n=0}^{N-1} x(n)\right]/TN(N^2-1) \tag{8}$$

Generally, the foregoing treatments of data should be applied, if possible, to the processed data; i.e., the data that have been corrected for sensor response and the system transfer function. Some NEMP test data require integration, such as, the electric and magnetic free-field sensor data. Usually, this is accomplished by hardware. However, software implementation is possible provided detrending procedures are used. If Fourier transforms of the data are required, then the detrending of the data should be performed before a transform algorithm is implemented.

2.5 NORMS

Time-domain responses to NEMP illumination are varied and are, in general, quite complex. In an attempt to identify a minimum of set of system response parameters, certain norms have been suggested (Ref. 5). These include the following norms for each system's time response:

$$\left|x(t)\right|_{\substack{\text{max.over}\\ \text{all } t}} \qquad \text{PEAK VALUE} \tag{9}$$

$$\left|\frac{d}{dt}x(t)\right|_{\substack{\text{max. over}\\ \text{all } t}} \qquad \text{PEAK RATE OF RISE} \qquad (10)$$

$$\left|\int_{-\infty}^{\infty} x(t')dt\right|_{\substack{\text{max. over}\\ \text{all } t}} \qquad \text{IMPULSE} \qquad (11)$$

$$\int_{-\infty}^{\infty}|x(t')|\,dt' \qquad \text{RECTIFIED IMPULSE} \qquad (12)$$

$$\int_{-\infty}^{\infty}|x(t')|^2dt'^{1/2} \qquad \text{ACTION INTEGRAL NORM} \qquad (13)$$

$$\int_{-\infty}^{\infty}|x(t')|^2dt' \qquad \text{ACTION INTEGRAL*} \qquad (14)$$

It is clear that the norms will be sensitive to sampling, filtering, noise, and data trends. These topics are investigated by considering certain NEMP-like response data with additive White-Gaussian noise combined with different sampling intervals.

2.6 COMPOSITE WAVEFORMS

For the fast transient signals induced by NEMP testing, digitizers based on CRT scan converter technology have been used. These devices provide a record length of only 512 samples. Consequently, the sampling rate required to capture the high frequency content does not provide sufficient resolution bandwidth (Refs. 2 and 4). In order to compensate for this lack of resolution, more than one digitizer is used with time delay in triggering to record the waveform. Typically, three digitizers are used in a sequenced triggering scheme with some overlapping in the recorded signals and with different

*The action integral is not truly a norm according to the mathematical definition of norms.

sampling rates. A composite signal is formed by using an interpolation scheme such as spline interpolation to tie the signals from the individual recorders. Testing algorithms have been developed to evaluate the veracity of the results (Ref. 6).

Recently, a digitizer was developed that uses a demultiplexing scheme and arrays of charged-coupled devices (CCD) to achieve very high sampling rates (≤1.348 gigasamples/s) and a long record length (10,240 samples) with a resolution of 8 bits (Ref. 7). This device would obviate the need for using composite waveforms for most applications. However, they have not been available for enough time to be employed extensively.

Since the existing NEMP test data have been collected in composite records, there is a need for quantitating the effects of forming composite records. This may be accomplished by simulating the process of forming composite records while using general analytical data with added White-Gaussian noise. This study is currently underway.

3.0 NUMERICAL RESULTS

The study of the accuracy and limitations of digitizing test transient data is conducted by considering three analytically derived generic time-domain waveforms. In general, the system response data for NEMP illumination can be expressed as superposition of damped sinusoids; i.e.,

$$x(t) = \sum_{\alpha=1}^{N_p} C_\alpha e^{S_\alpha t} + \text{complex conjugates}$$

$$= 2 \sum_{\alpha=1}^{N_p} |C_\alpha| e^{+\sigma_\alpha t} \cos(j\omega_\alpha t + \phi_\alpha) \qquad (15)$$

where

$x(t)$ = sample of response as a function of time
N_p = number of complex poles
C_α = complex residues
S_α = complex poles
t = time
$|C_a|$ = absolute value of the complex residues
e = 2.71828
σ_α = attenuation constant
ω_α = resonant radian frequency
$j = \sqrt{-1}$
ϕ_α = phase

Consequently, the three generic data sets, A, B, and C are expressed in terms of poles and residues in Tables 1, 2, and 3, respectively.

TABLE 1. Data set A, simulating data for small aircraft system.

α	$\lvert C_\alpha \rvert$	ϕ_α	σ_α	$\omega_\alpha/2\pi$
1	240	18°	-9.9×10^6	8.7×10^6
2	38	216°	-19×10^6	27×10^6
3	19	48°	-25×10^6	45×10^6

TABLE 2. Data set B, simulating data for a medium aircraft system.

α	$\lvert C_\alpha \rvert$	ϕ_α	σ_α	$\omega_\alpha/2\pi$
1	240	71°	-4.0×10^6	3.5×10^6
2	38	-126°	-7.5×10^6	11×10^6
3	19	42°	-9.9×10^6	1.8×10^6

TABLE 3. Data set C, simulating data for a large aircraft system.

α	$\lvert C_\alpha \rvert$	ϕ_α	σ_α	$\omega_\alpha/2\pi$
1	0.27	-90°	-0.65×10^6	2.0×10^6
2	0.31	-90°	-1.7×10^6	3.6×10^6
3	0.63	-90°	-1.1×10^6	5.5×10^6
4	0.79	-90°	-1.6×10^6	8.9×10^6

NOTE:

$\lvert C_\alpha \rvert$ = Absolute value of the complex residues (amplitude)
ϕ_α = Phase
σ_α = Damping coefficient
$\omega_\alpha/2\pi$ = Frequency

White-Gaussian noise with a zero mean value is added to the data. The resulting SNR is defined:

$$SNR = \frac{\text{peak signal}}{\text{standard deviation of noise}} \tag{16}$$

In Figs. 3 through 7, two noise levels are considered with the generic data sets and the resulting Fourier transforms are exhibited. These data are followed by Figs. 8 through 13 where the effects of sampling rates are presented. And finally, Figs. 14 through 19 present the combined effects of noise and sampling. The selections of noise levels and sampling rates were made to coincide with those of recent NEMP tests. The transformed data are plotted up to the Nyquist folding frequency for the respective sampling rates. Clearly, the minimum requirements for accurate data from 500 kHz to 100 MHz require that:

$$SNR > 30 \text{ dB} \tag{17}$$

$$T < 2 \text{ ns} \tag{18}$$

$$NT > 2 \ \mu s \tag{19}$$

where

T = sampling interval
N = total number of data samples

This is also seen in Figs. 20 through 27 where corresponding time-domain results are exhibited.

Treatment of data with digital filtering and detrending can improve their quality. This is shown in Figs. 20 through 39. A ramp trend is introduced into each of these data set and the turnon time is set a zero. The time-domain graphs (Figs. 28 through 33) clearly exhibit the ramp trend before and after detrending. However, caution is needed in using the detrending procedure on signals where the record length is less than the signal duration. Severe signal distortion may occur in this situation.

The spectral effects of trends are shown in Figs. 34 through 39. Two prominent effects are easily seen. First, the trend introduces an anomalous low frequency spectral content; and second, the termination of the ramp at the end of the record introduces a spurious high frequency spectrum. However, with the trend removed, the spectrum becomes more accurate. A comparison of the detrended signal in Fig. 34 with the original signal spectrum in Fig. 3 shows some differences. This results from the use of an extremely low frequency signal component added to the data to introduce the trend; whereas, the trend was removed by using a least-squares fit to a straight-line trend.

Norm data are best presented in tabular form. Tables 4 and 5 present typical results for norm calculations from noisy and undersampled data. As might be expected, with a moderate noise level, SNR $\geq$ 20 dB, little error was introduced into the peak value. The impulse and action integral norms exhibit moderate errors. However, the peak rate-of-rise and rectified impulse norms exhibit substantial errors (up to 666 percent). Also, the noise tended to increase the norm values. For severe noise levels; i.e., SNR < 10 dB, very large errors are observed. These errors are sufficiently large that the norm calculations are not valid. It also appears that the norm errors are sensitive to the waveshape. The peak norm appears to be least affected by the errors.

The undersampling of data tended to provide substantial errors in the rate-of-rise norms. However, the other norms were not affected as much. In general, undersampling resulted in reduced norm values.

TABLE 4. Small aircraft external response norm errors (%).

SAMPLE INTERVAL/SNR	PEAK	PEAK RATE OF RISE	IMPULSE	RECTIFIED IMPULSE	ACTION INTEGRAL
2 ns/30 dB	1.9	7.6	34.0	63.0	4.5
2 ns/20 dB	12.7	23.6	87.7	201.9	30.4
5 ns/∞	1.4	60.6	26.9	2.5	3.0
5 ns/30 dB	1.9	57.7	34.9	180.1	11.1
5 ns/20 dB	2.8	51.9	38.2	93.6	61.8
10 ns/∞	1.4	80.3	33.3	1.2	1.8
10 ns/20 dB	10.8	78.5	152.7	88.0	102.3

TABLE 5. Large aircraft internal response norm errors (%).

SAMPLE INTERVAL/SNR	PEAK	PEAK RATE OF RISE	IMPULSE	RECTIFIED IMPULSE	ACTION INTEGRAL
2 ns/30 dB	2.5	142.1	6.5	5.0	1.7
2 ns/20 dB	8.9	665.8	20.5	28.1	11.6
5 ns/∞	0.0	1.2	1.3	17.4	0.8
5 ns/30 dB	0.0	1.2	11.5	36.2	1.7
5 ns/20 dB	13.9	185.5	39.6	115.6	22.3
10 ns/20 dB	3.4	9.2	64.8	275.3	47.3

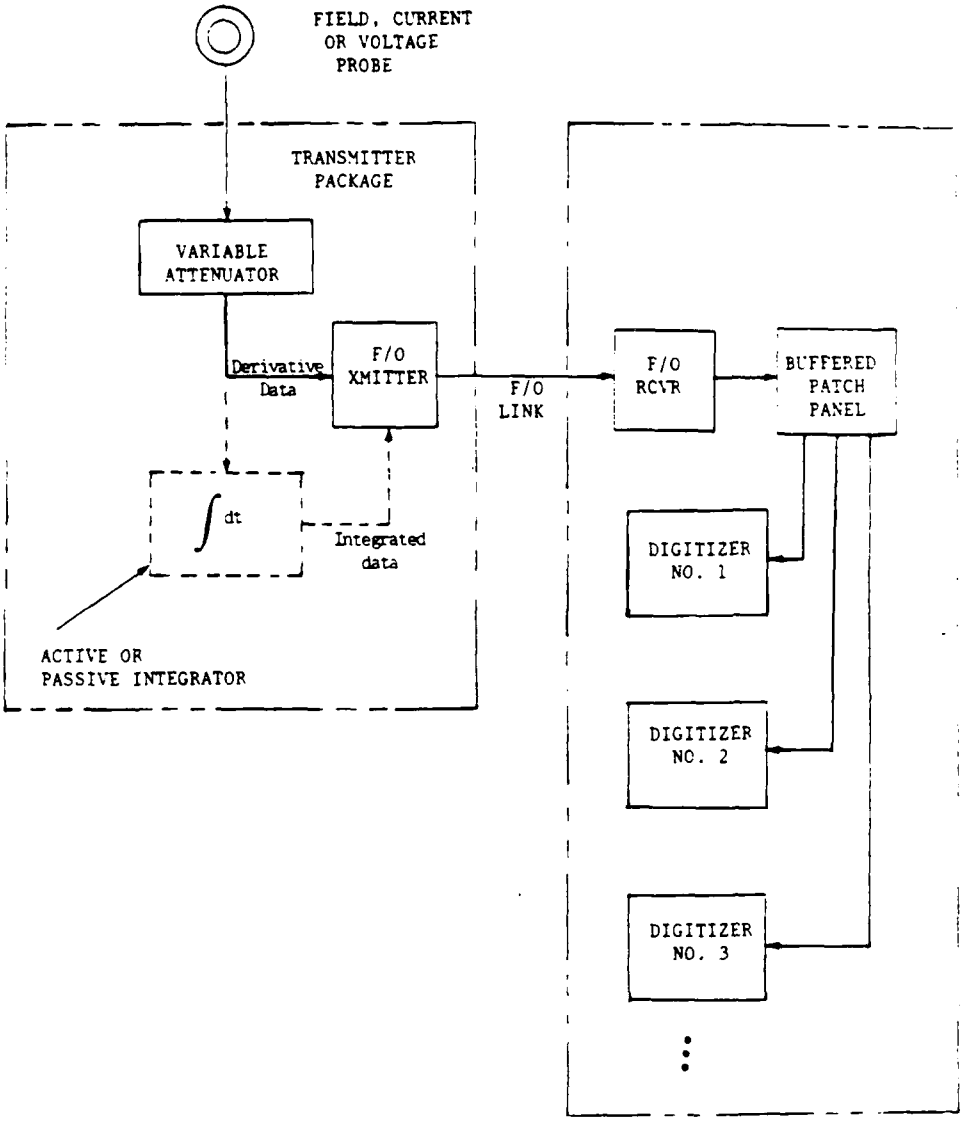

Figure 1. Typical system configuration for recording transient signals in NEMP testing.

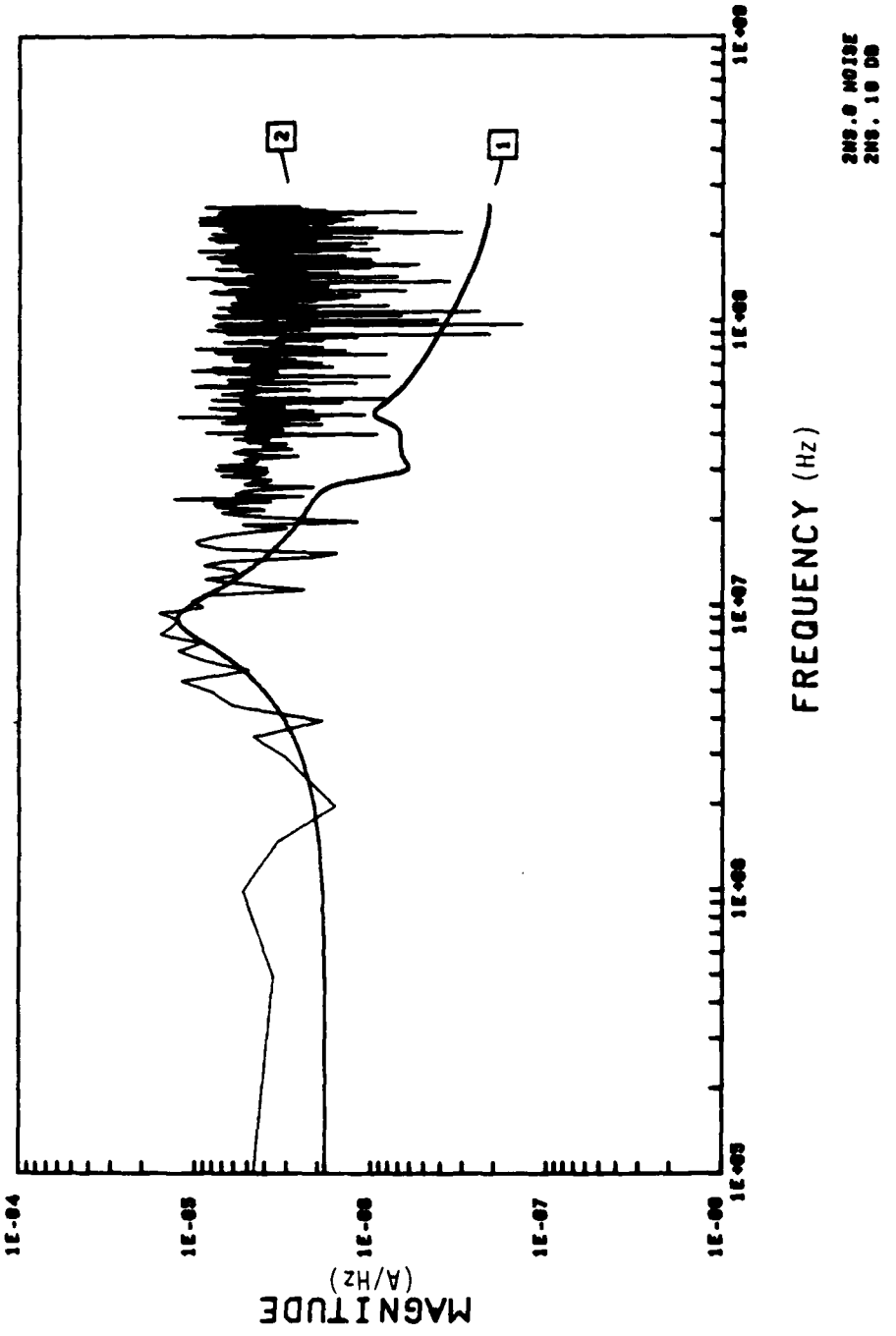

Figure 2. Small aircraft external response for a 2 ns sampling interval and 10 dB SNR.

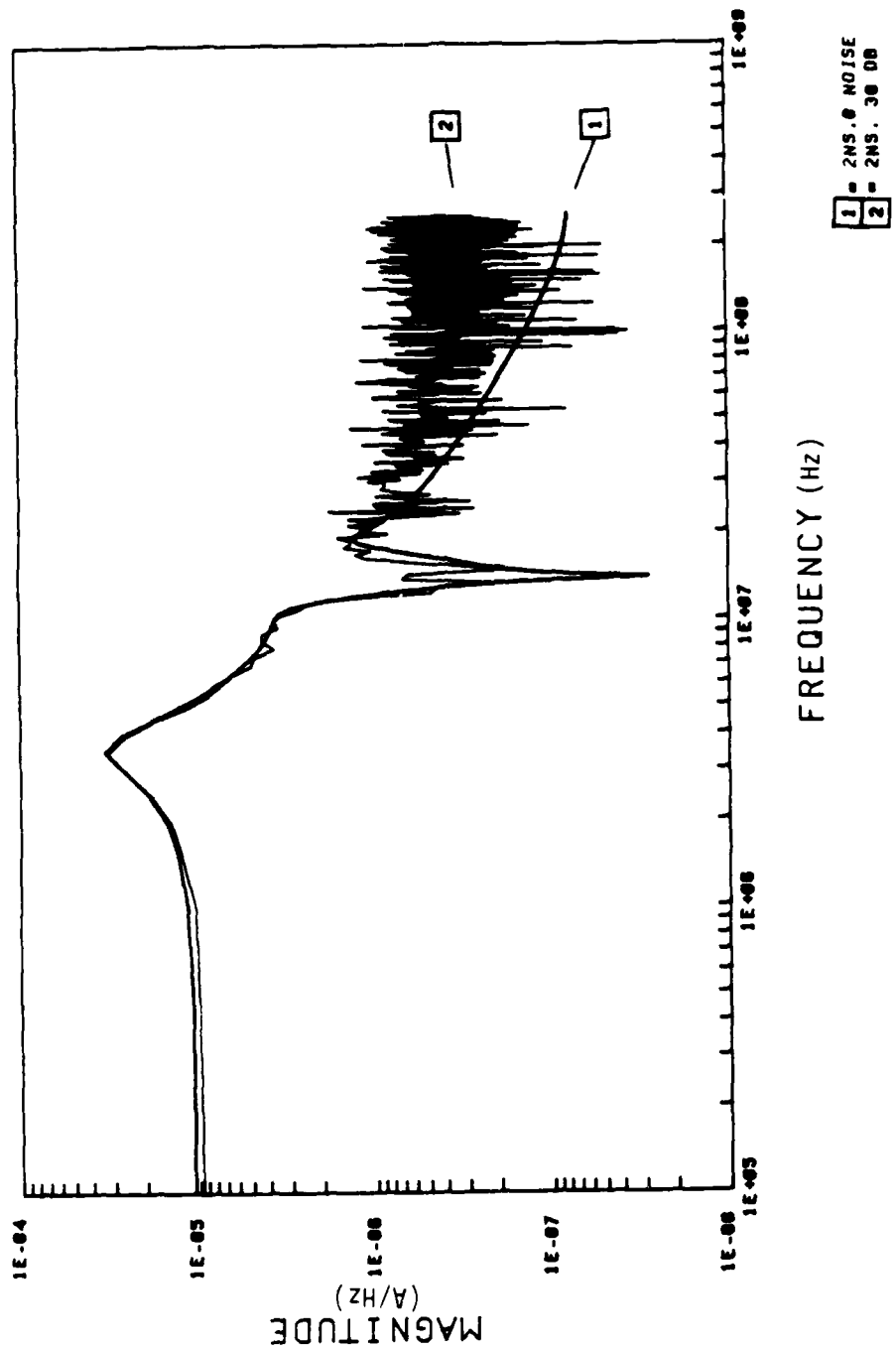

Figure 3. Large aircraft external response for a 2 ns sampling interval and 30 dB SNR.

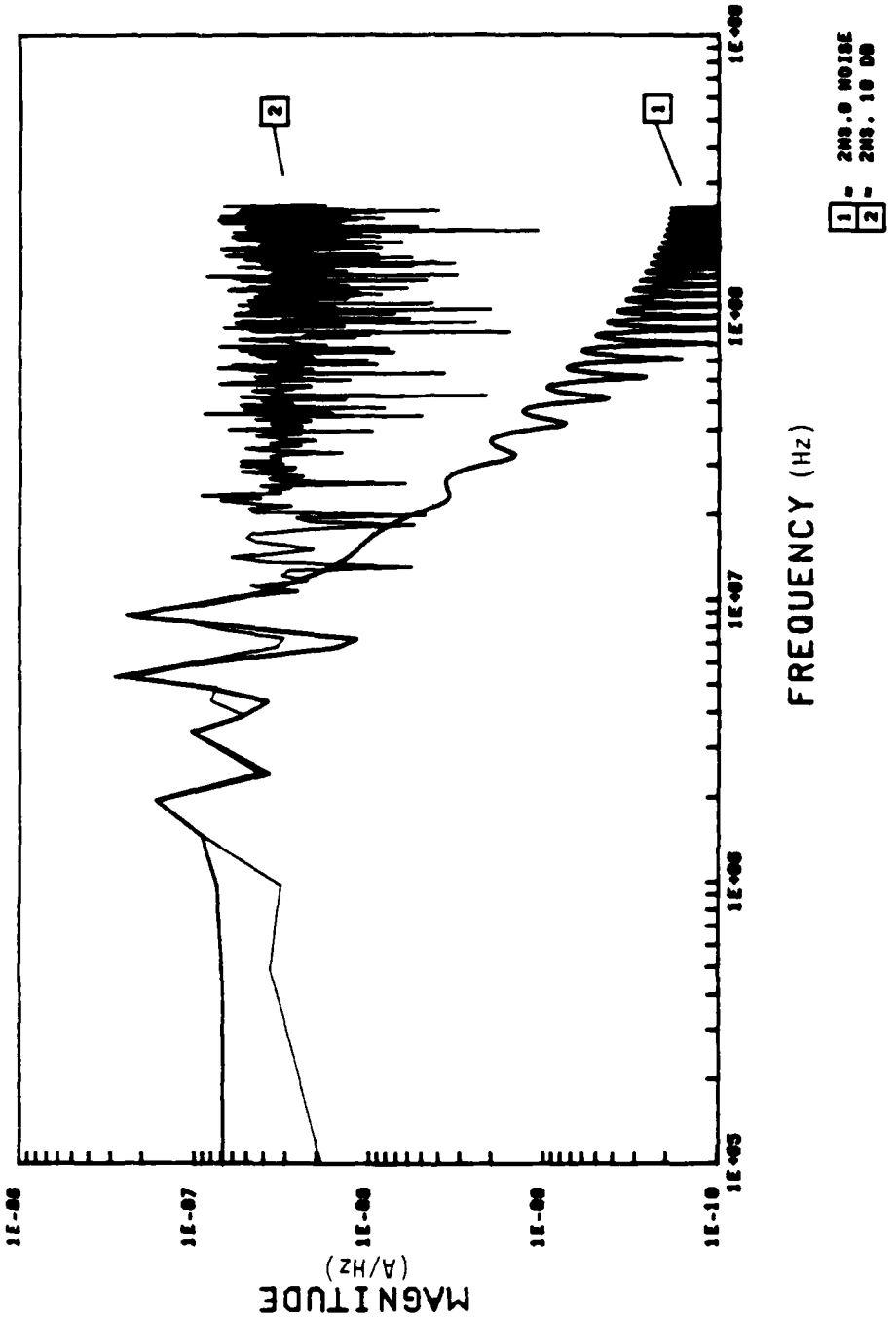

Figure 4. Large aircraft internal response for a 2 ns sampling interval and 10 dB SNR.

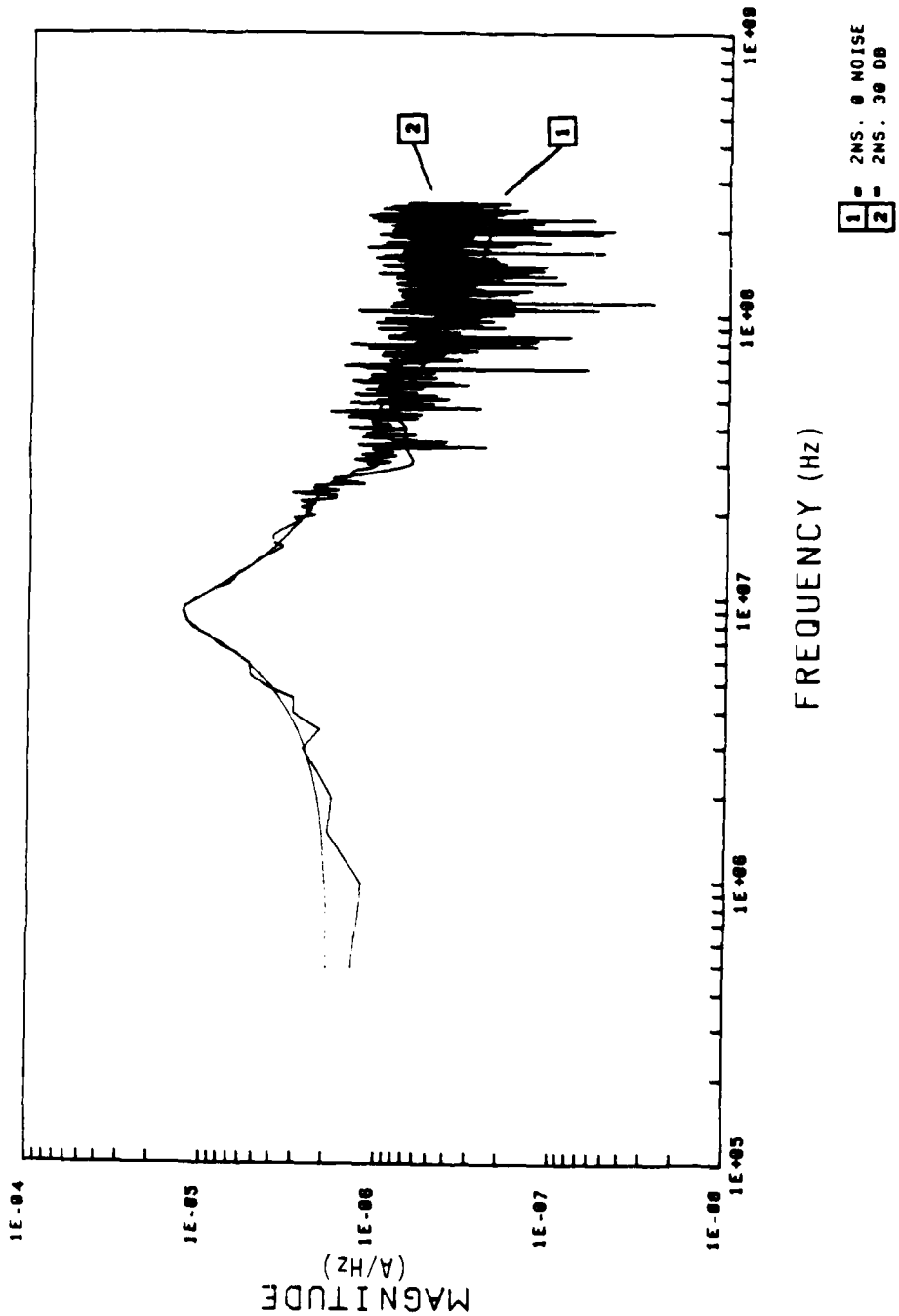

Figure 5. Small aircraft external response for a 2 ns sampling interval and 30 dB SNR.

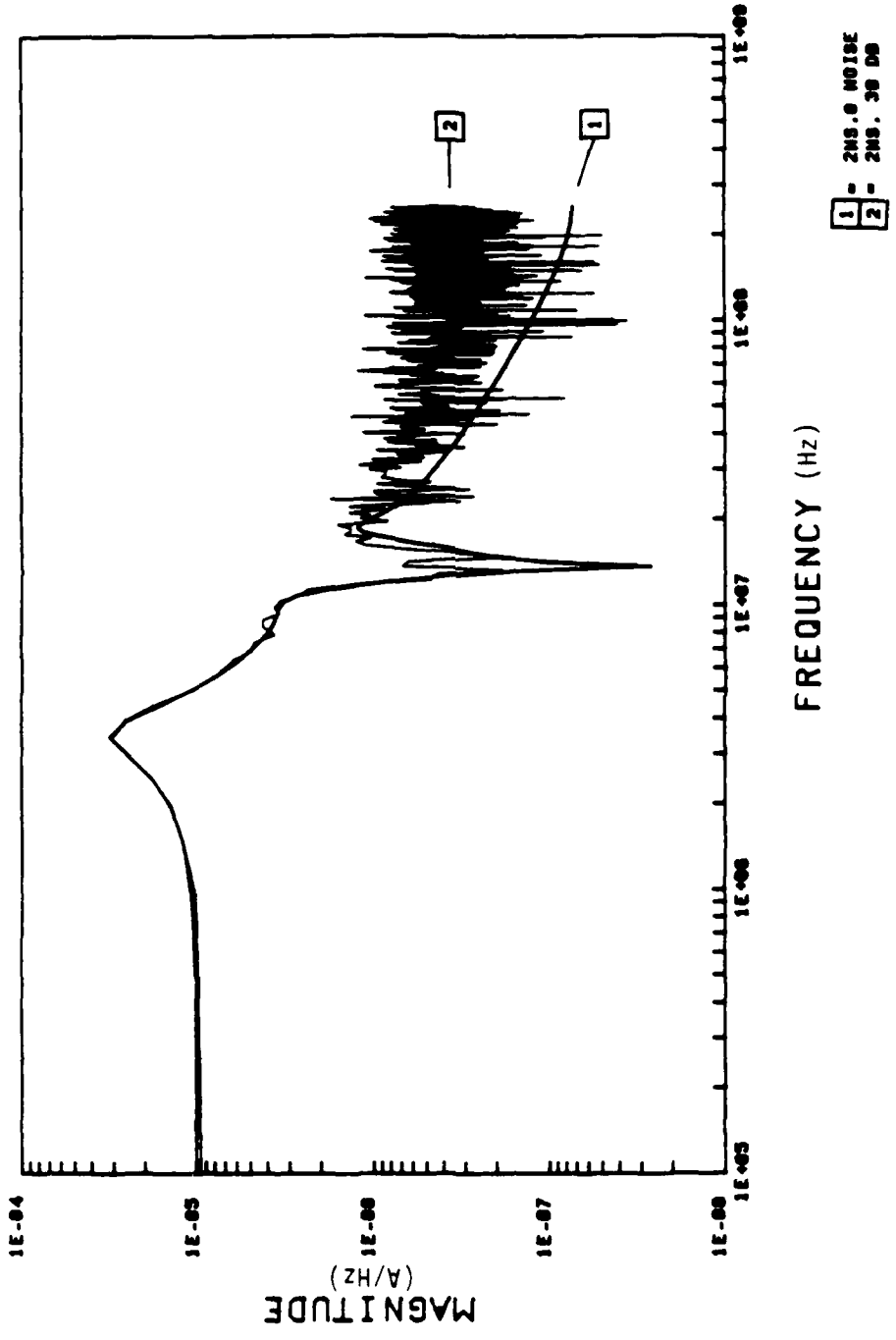

Figure 6. Large aircraft external response for a 2 ns sampling interval and 30 dB SNR.

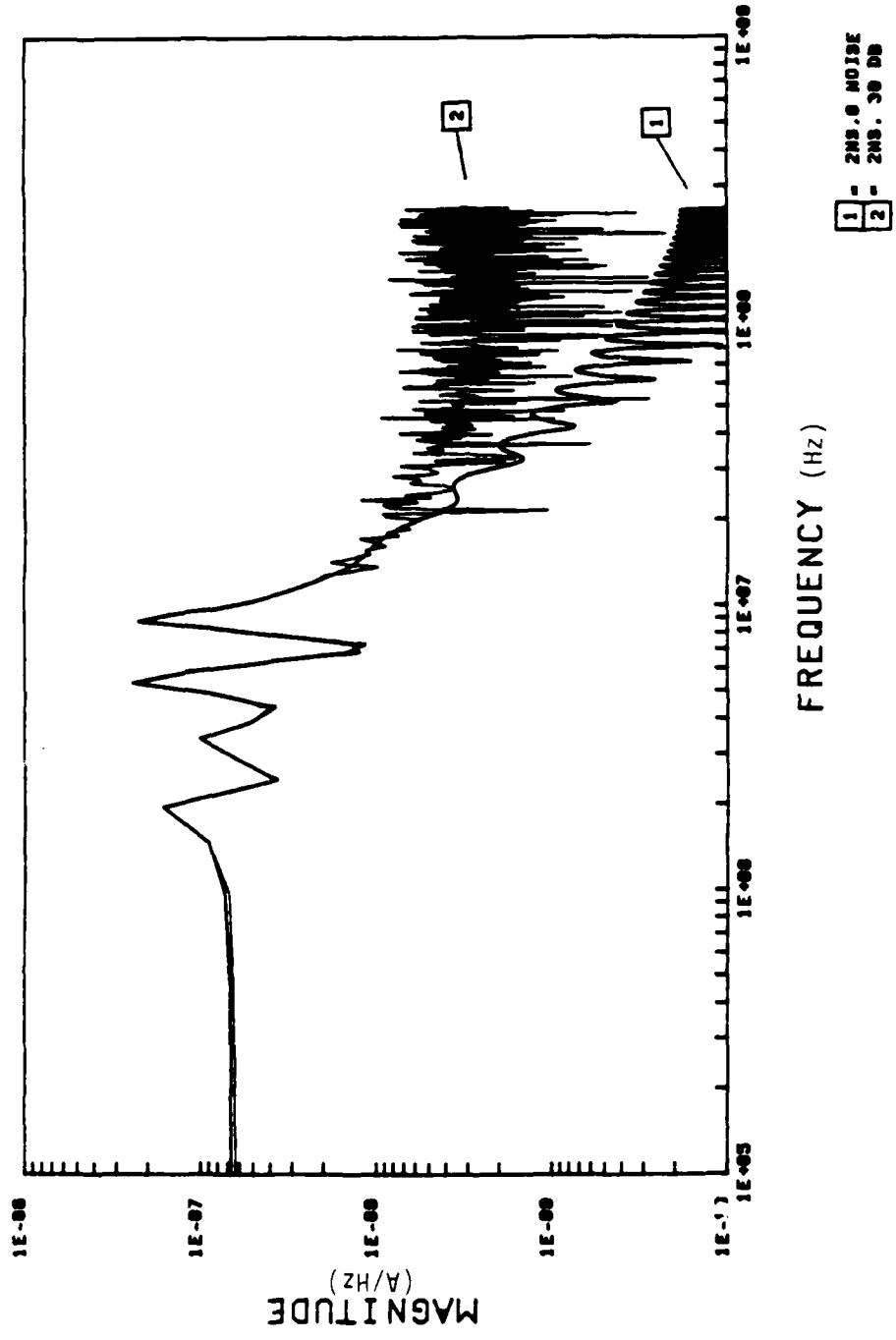

Figure 7. Large aircraft interior response for a 2 ns sampling interval and 30 dB SNR.

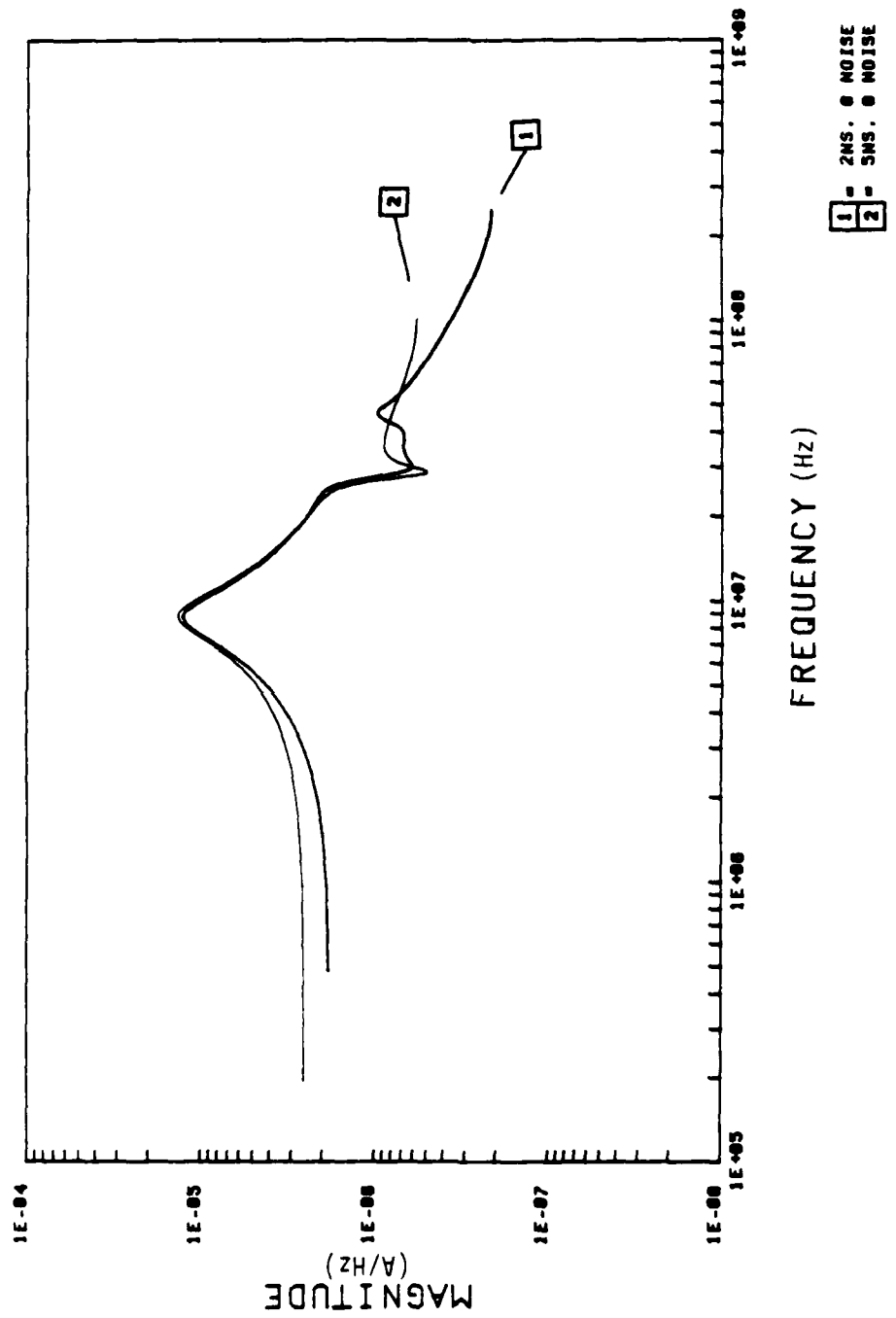

Figure 8. Small aircraft external response for 2 and 5 ns sampling intervals and ∞ dB SNR.

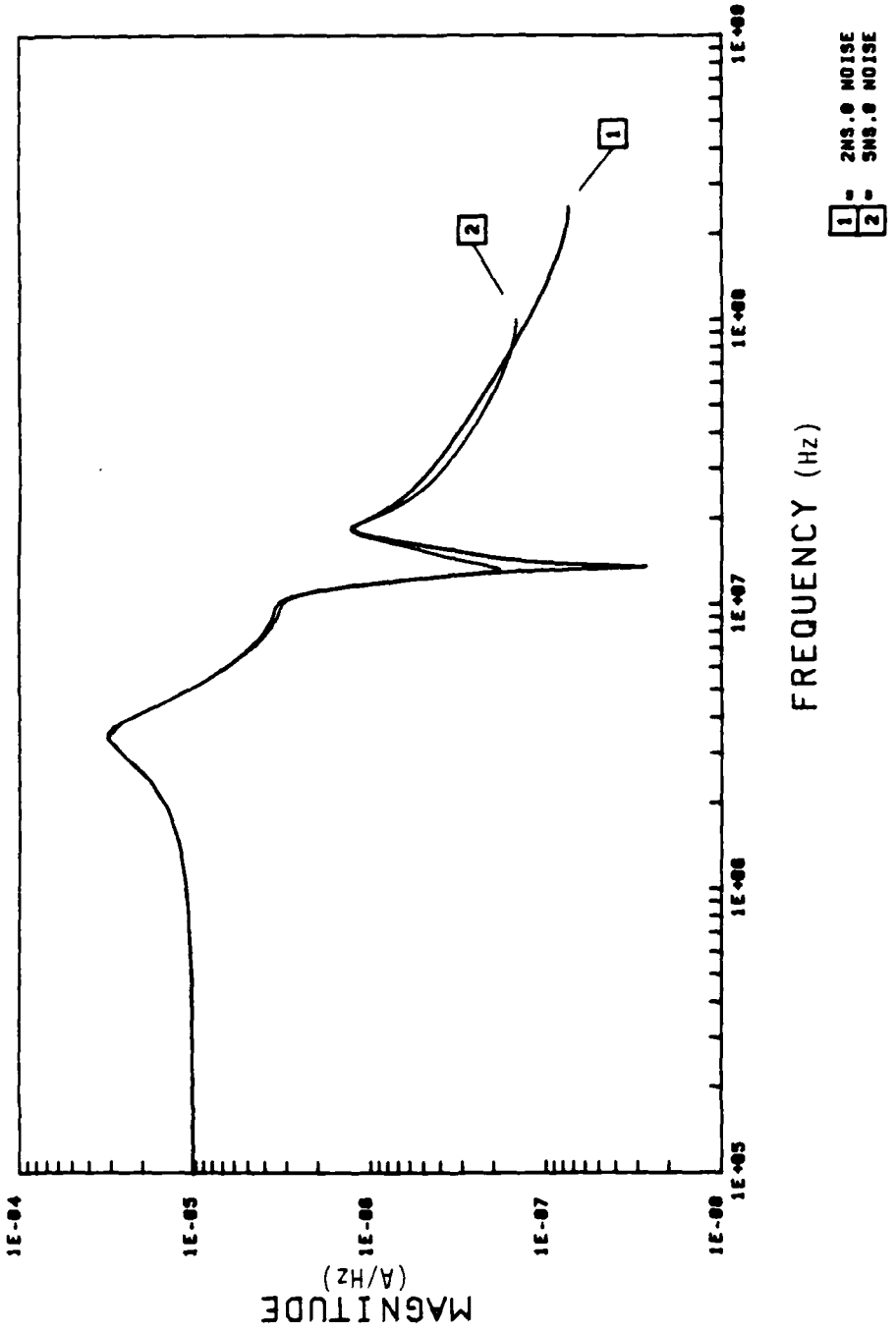

Figure 9. Large aircraft external response for 2 and 5 ns sampling intervals and ∞ dB SNR.

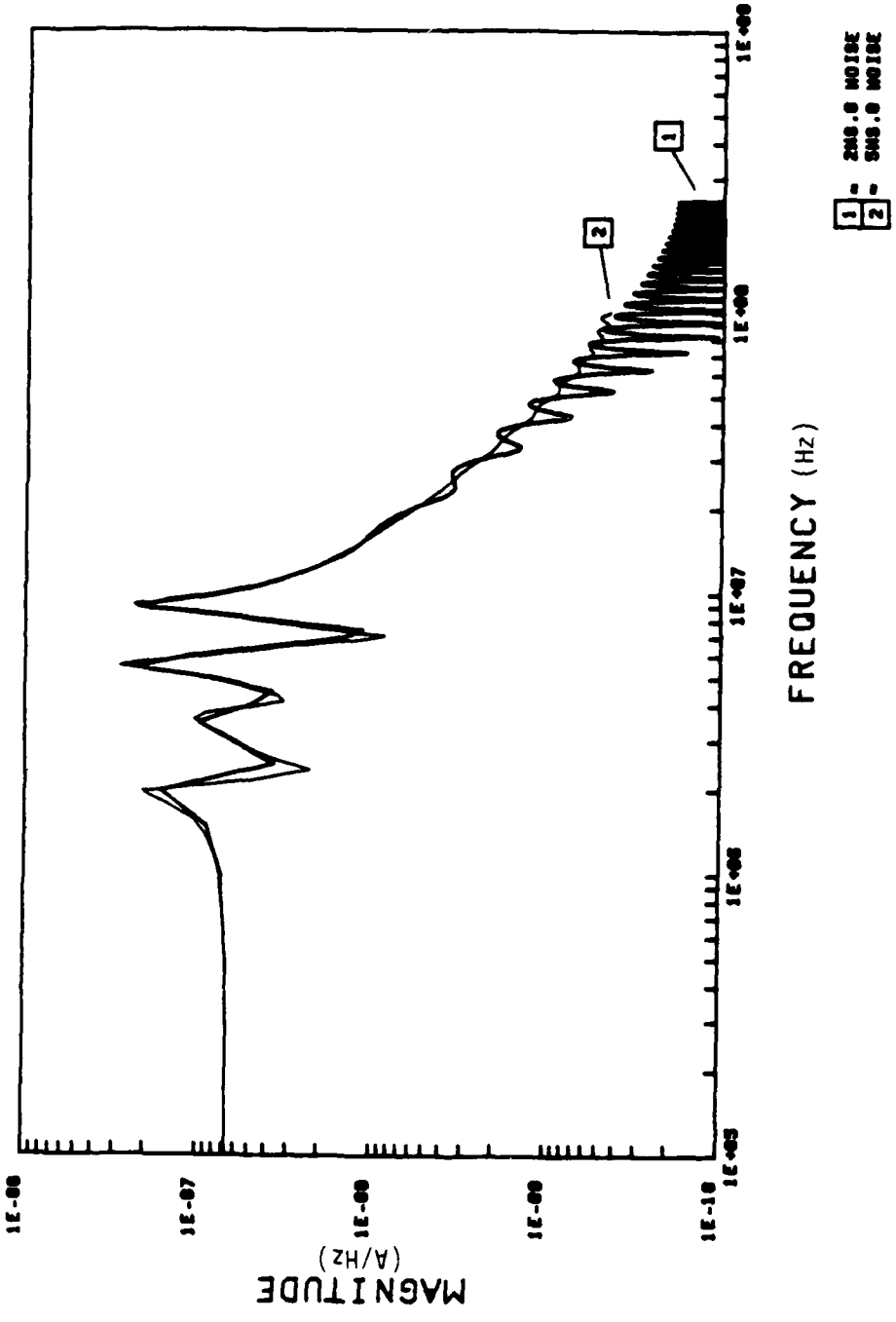

Figure 10. Large aircraft interior response for 2 and 5 ns sampling intervals and ∞ SNR.

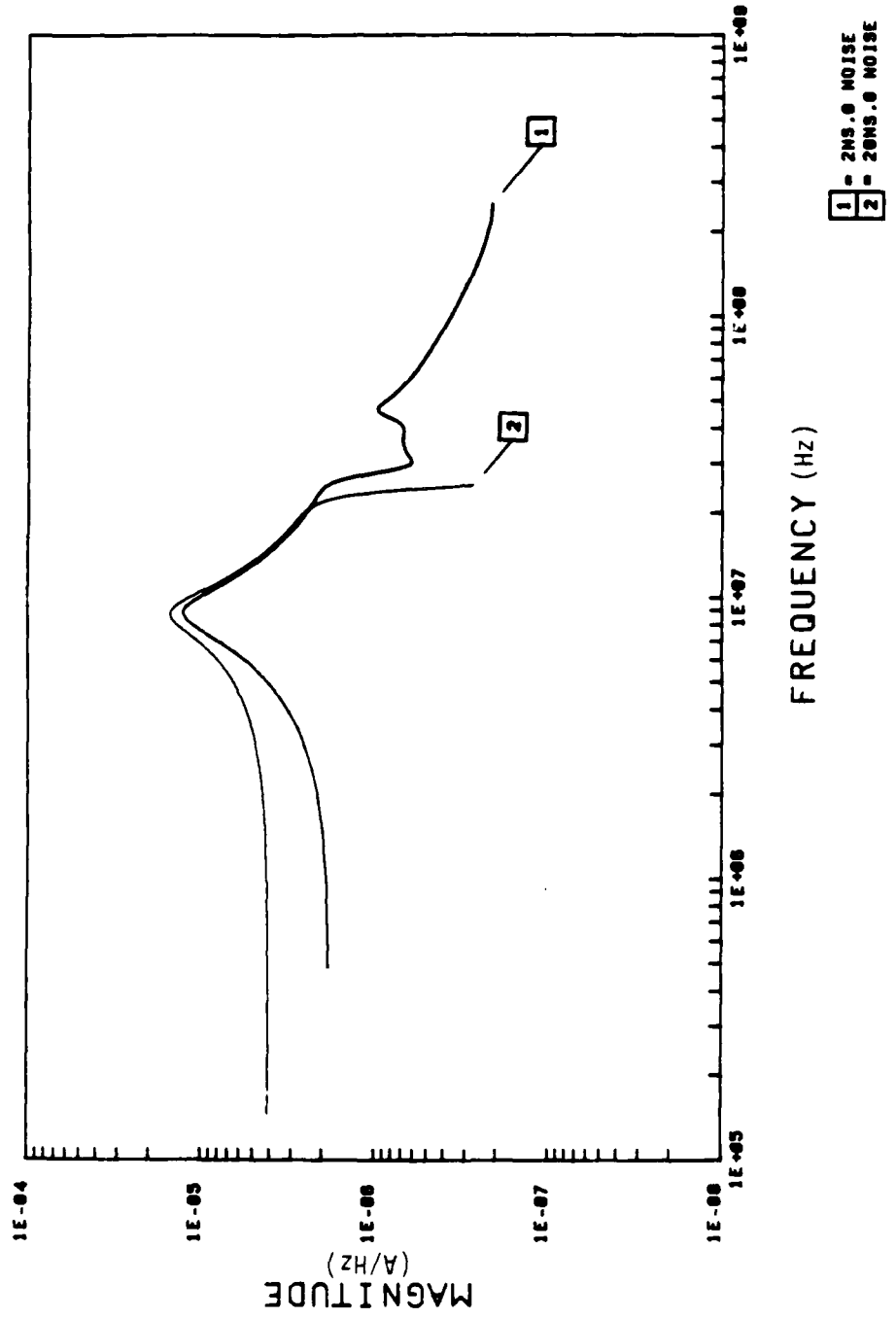

Figure 11. Small aircraft external response for 2 and 20 ns sampling intervals and ∞ dB SNR.

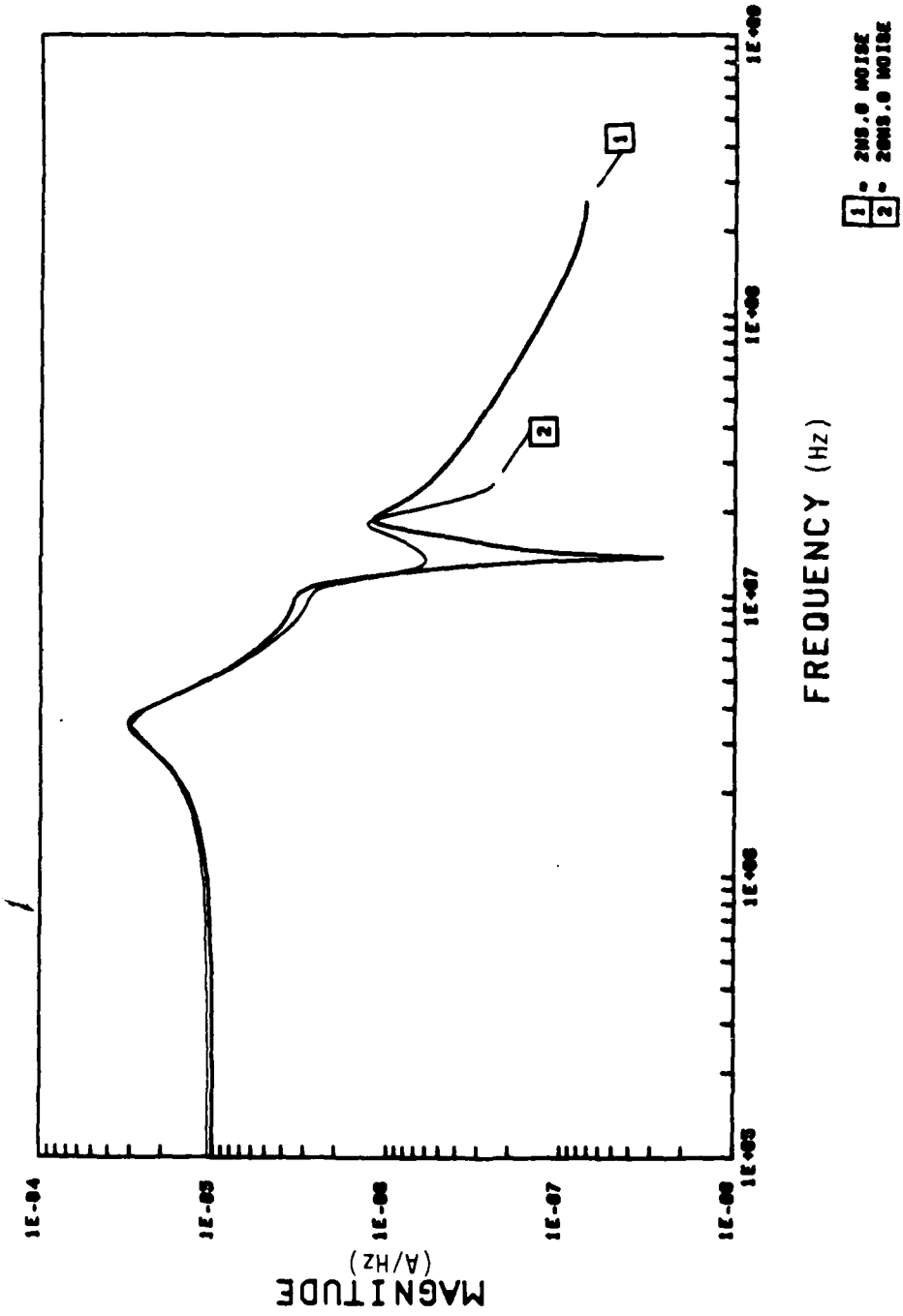

Figure 12. Large aircraft external response for 2 and 20 ns sampling intervals and ∞ dB SNR

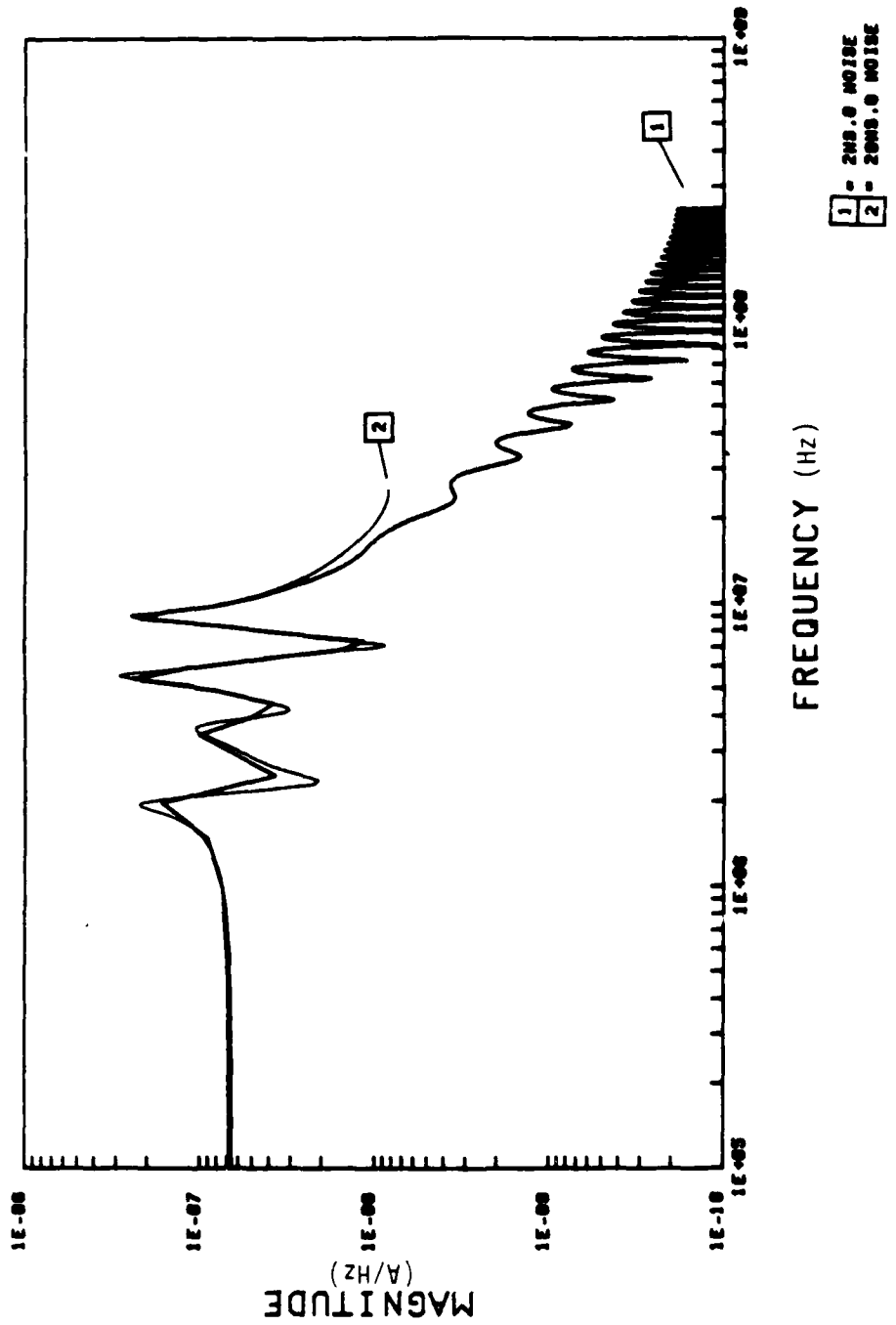

Figure 13. Large aircraft interior response for 2 and 20 ns sampling intervals and ∞ dB SNR.

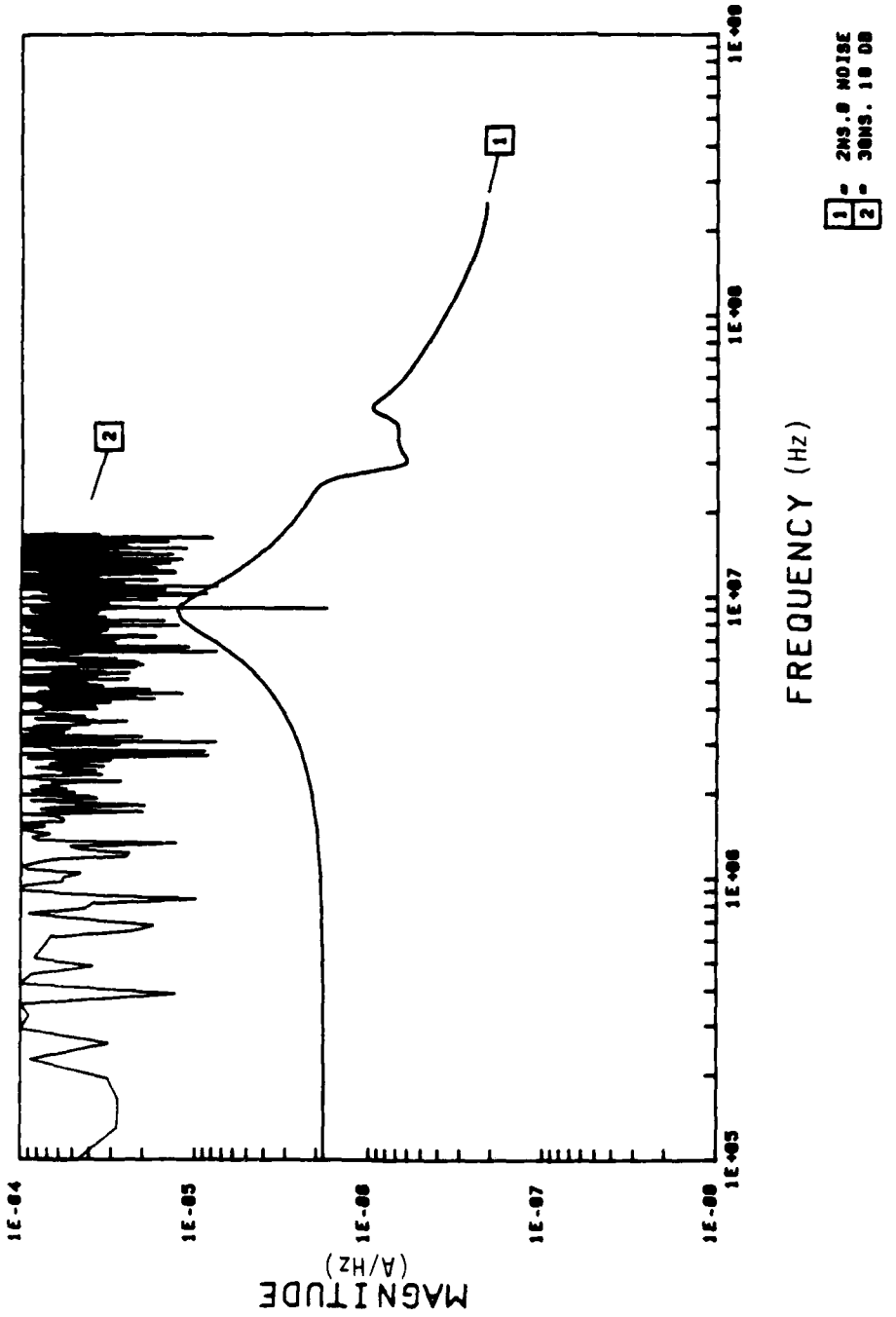

Figure 14. Small aircraft external response for 2 and 30 ns sampling intervals and 10 dB SNR.

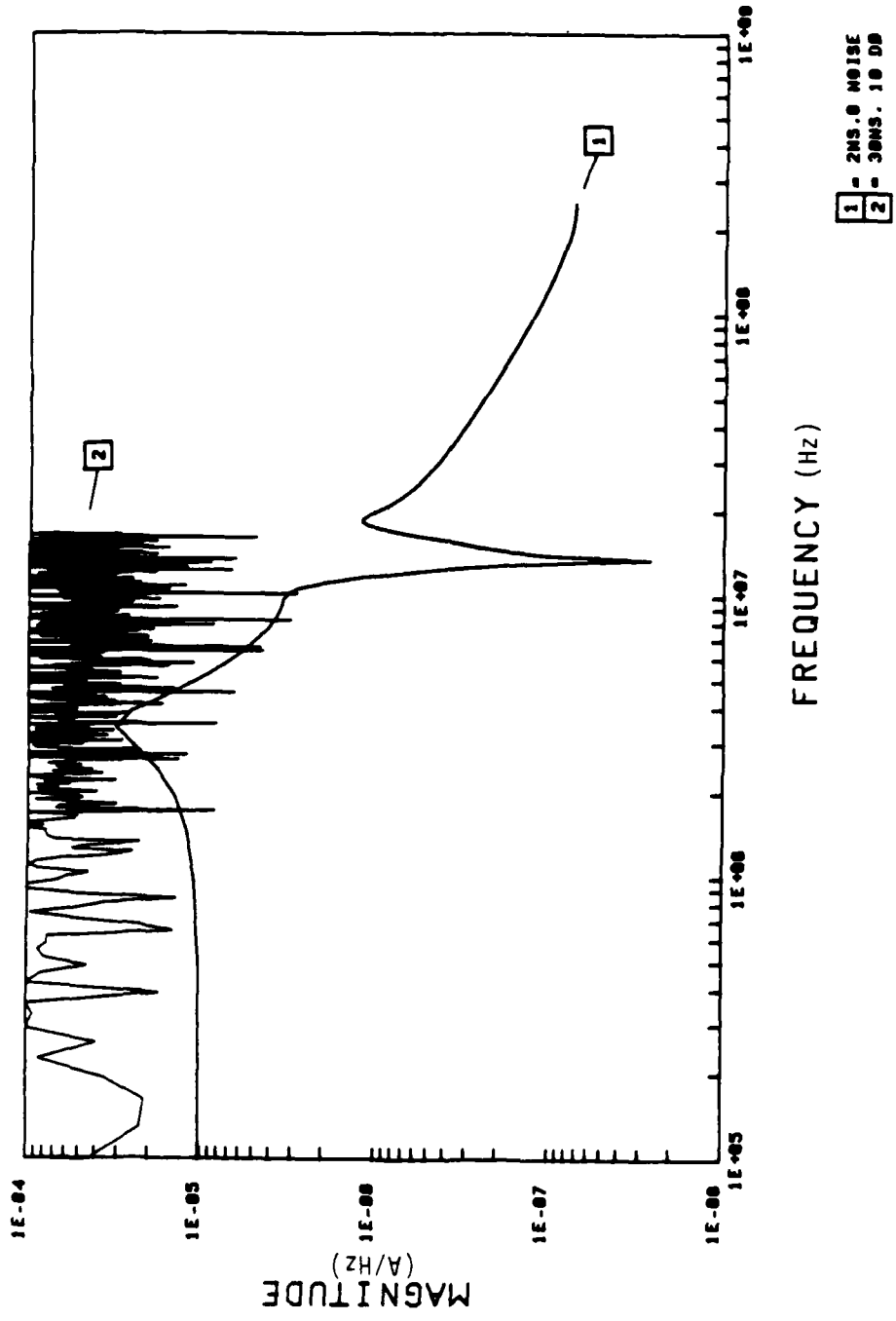

Figure 15. Large Aircraft external response for 2 and 30 ns sampling intervals and 10 dB SNR.

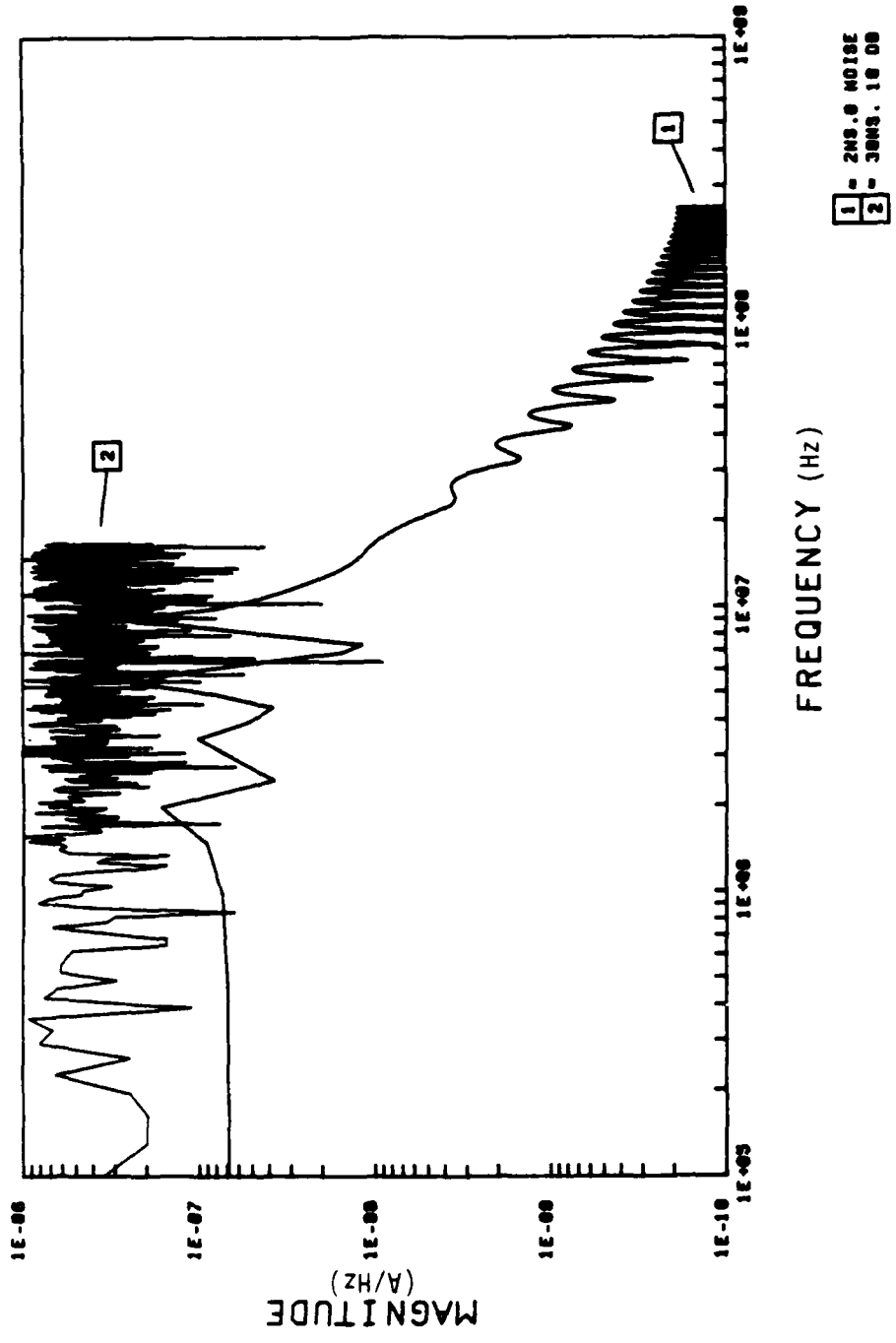

Figure 16. Large aircraft internal response for 2 and 30 ns sampling intervals and 10 dB SNR.

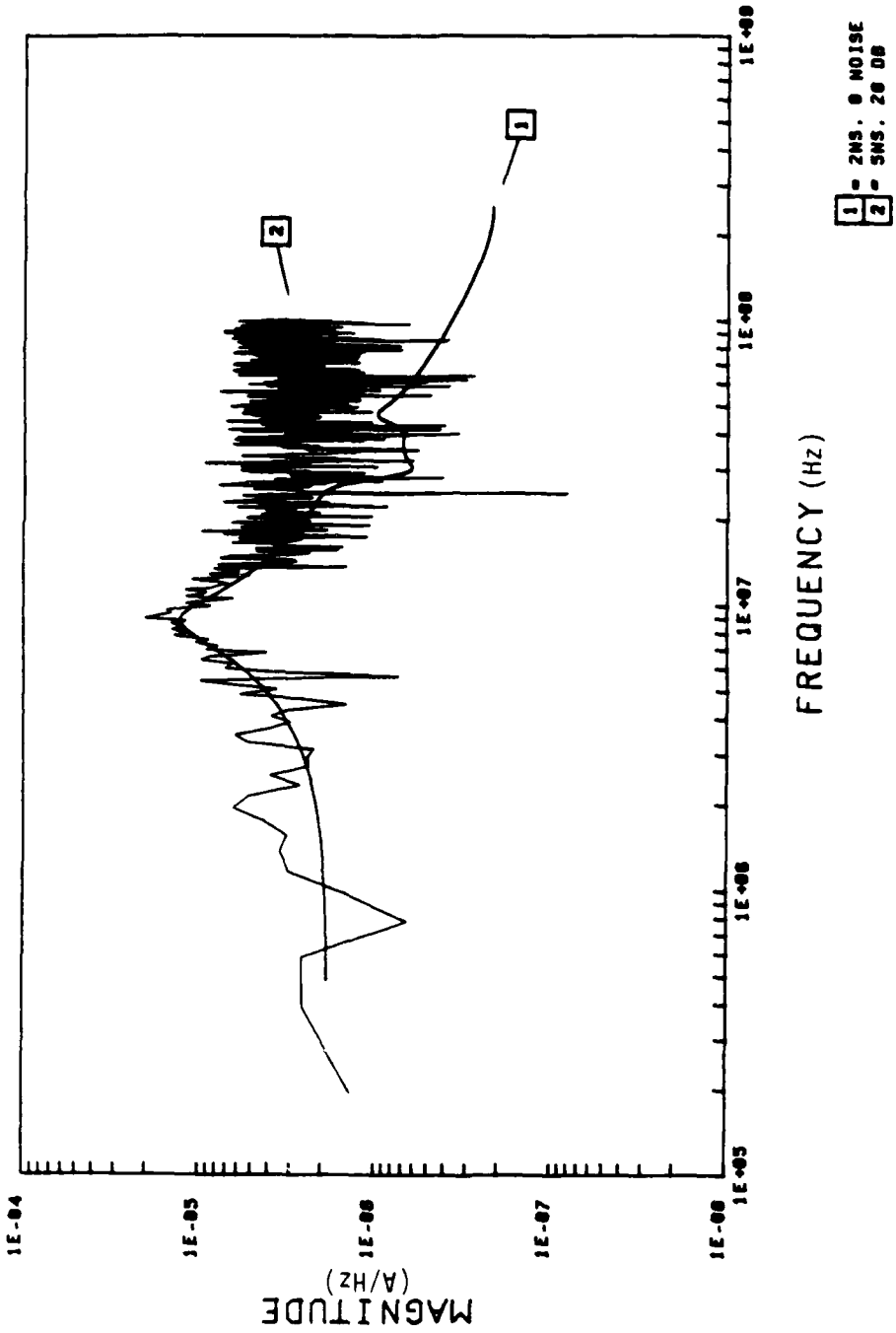

Figure 17. Small aircraft external response for 2 and 5 ns sampling intervals and 20 dB SNR.

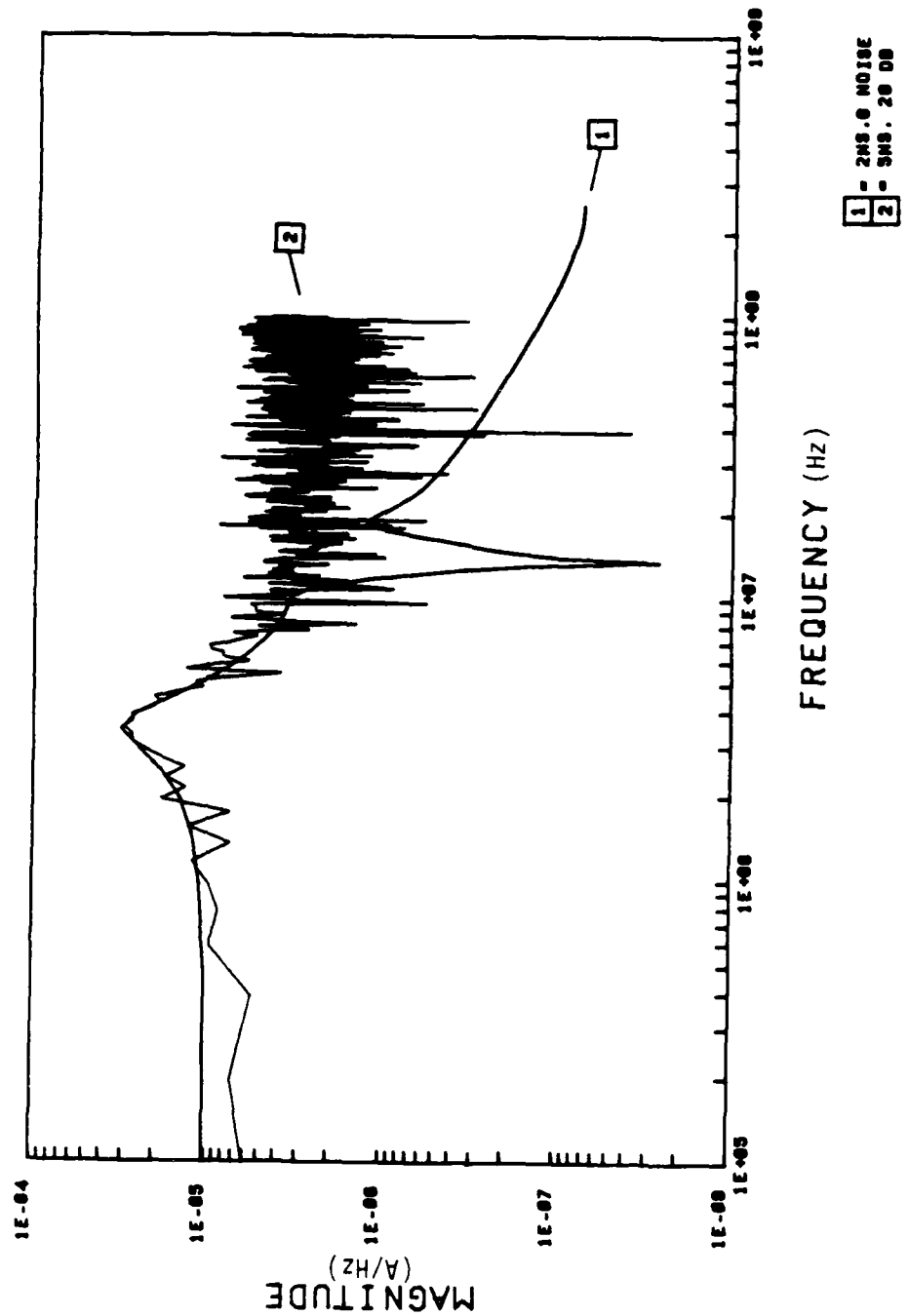

Figure 18. Large aircraft external response for 2 and 5 ns sampling intervals and 20 dB SNR.

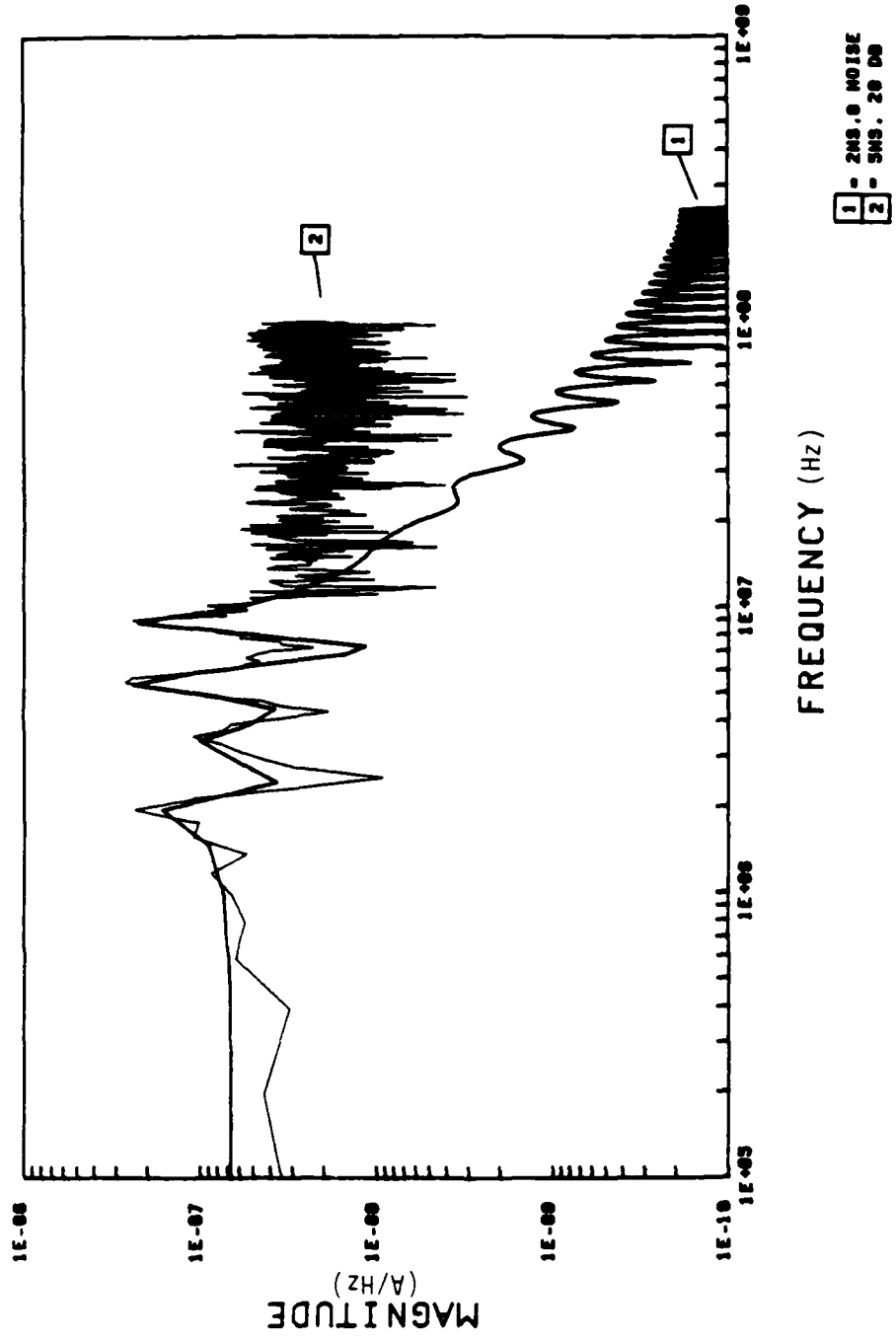

Figure 19. Large aircraft internal response for 2 and 5 ns sampling intervals and 20 dB SNR.

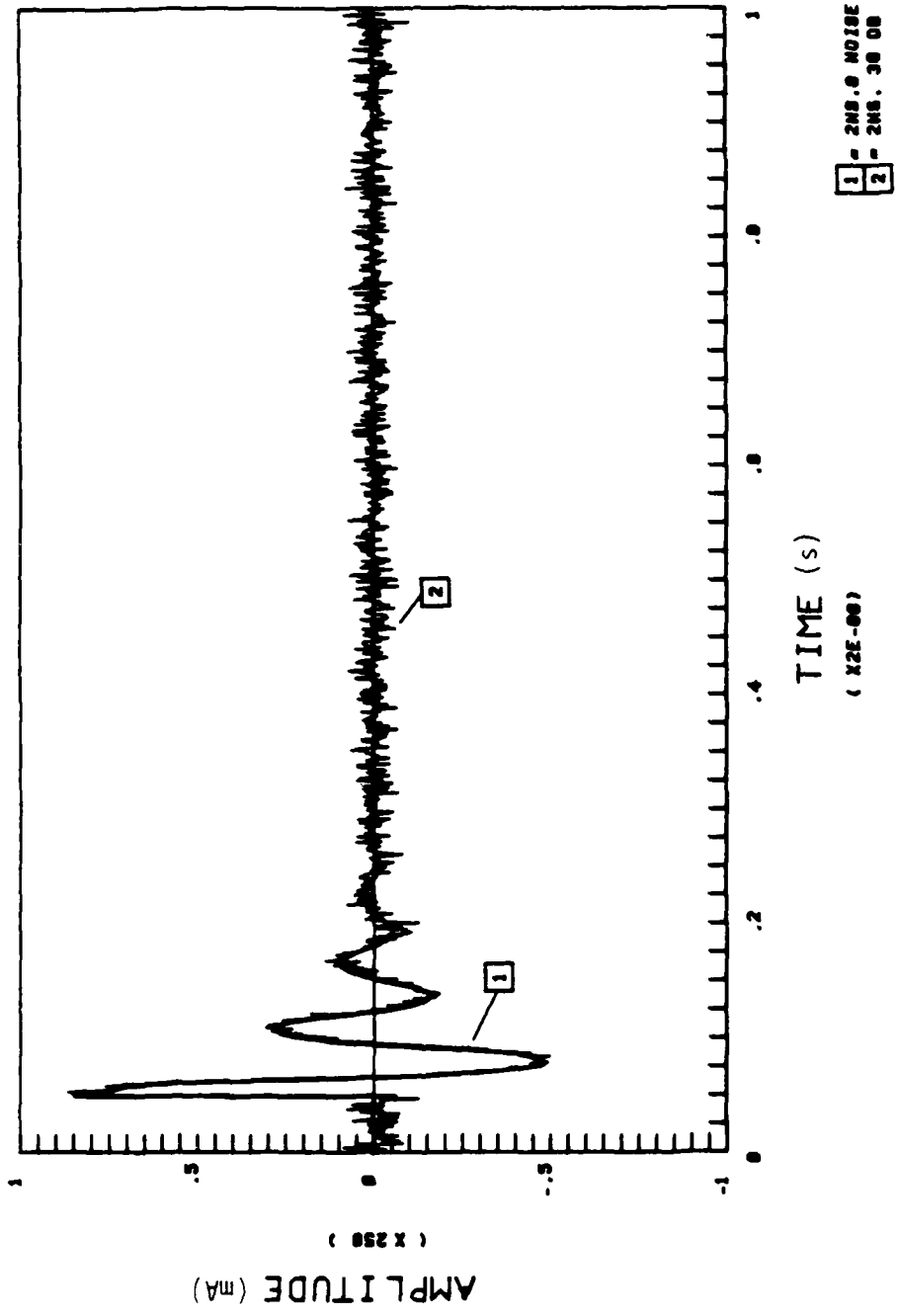

Figure 20. Small aircraft external time domain response for 2 ns sampling interval and 30 dB SNR.

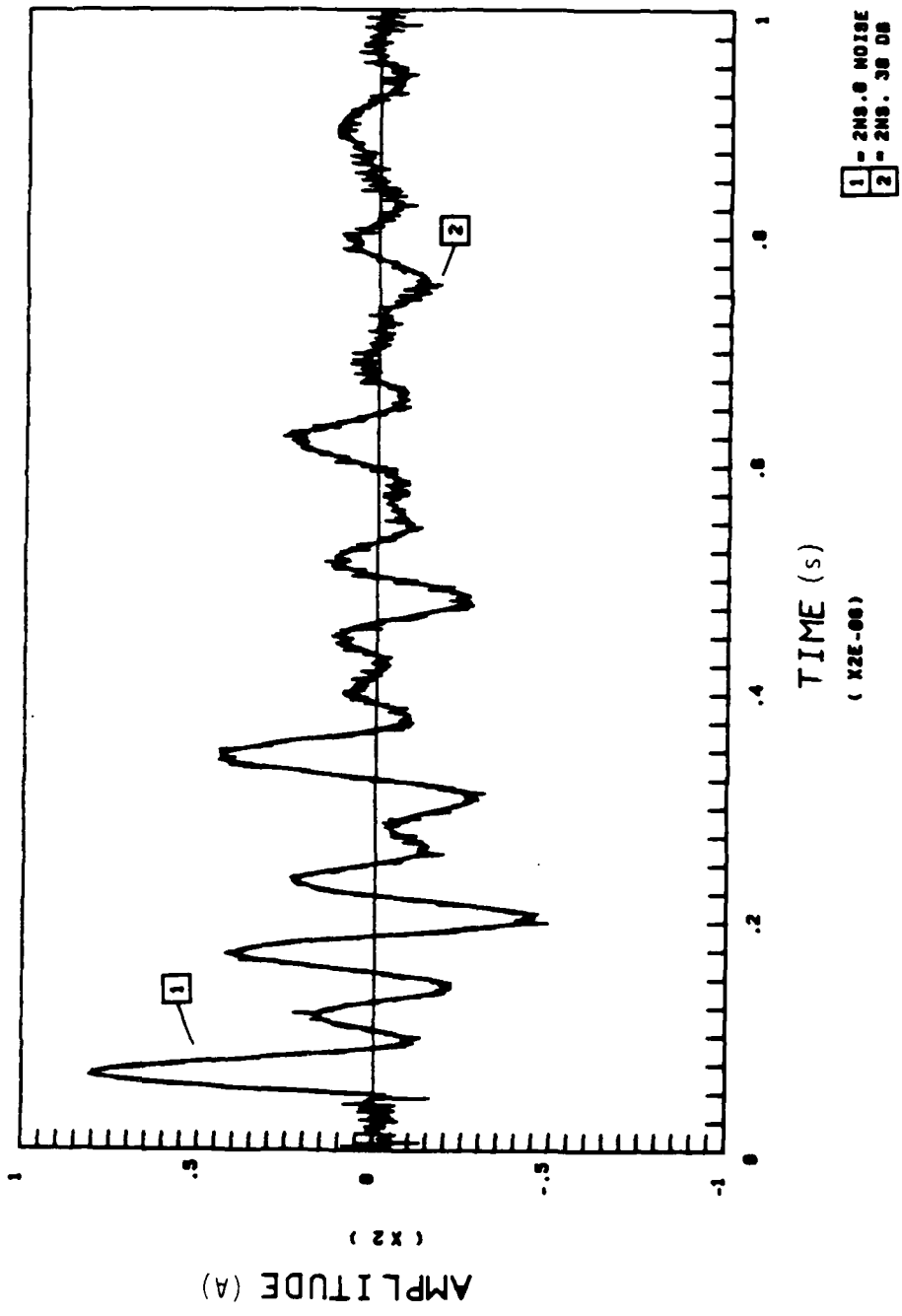

Figure 21. Large aircraft internal time domain response for 2 ns sampling interval and 30 dB SNR.

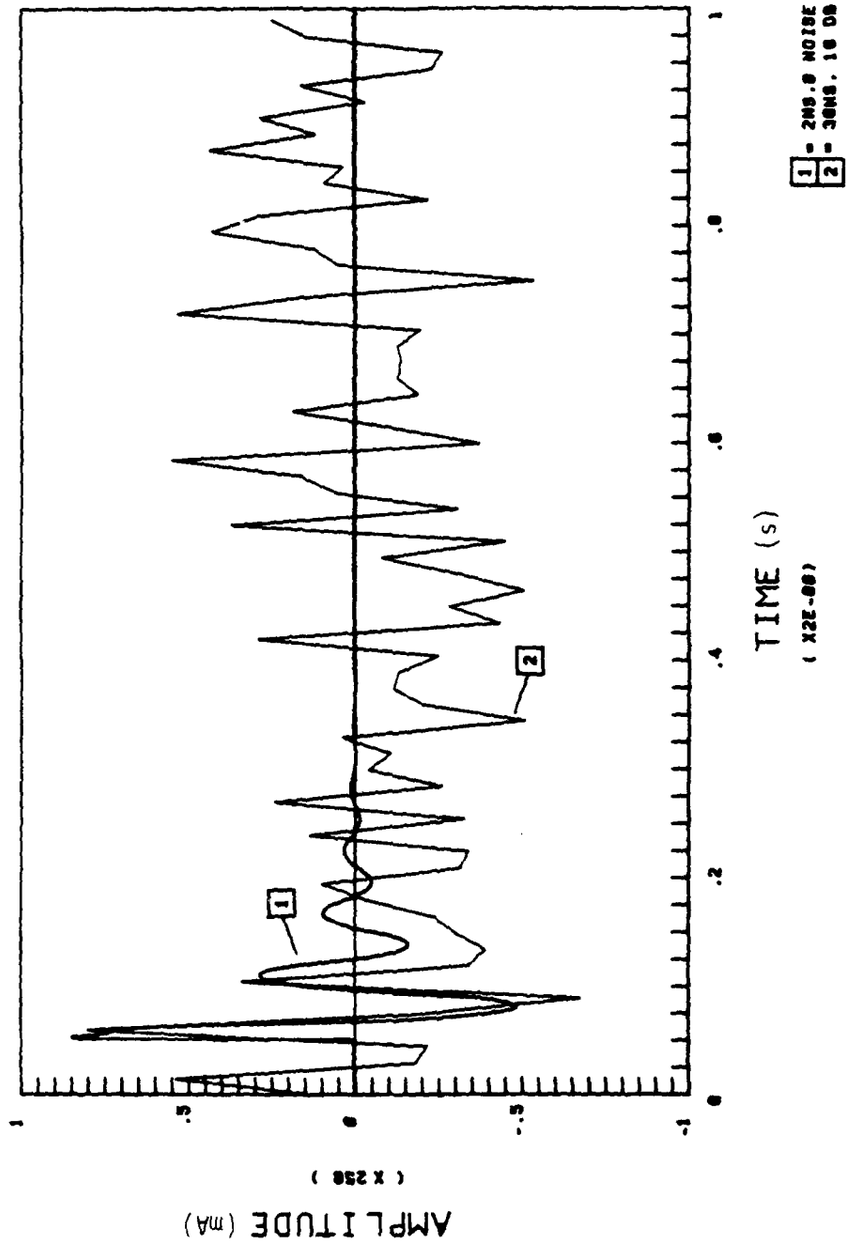

Figure 22. Small aircraft external time domain response for 2 and 30 ns sampling intervals and 10 dB SNR.

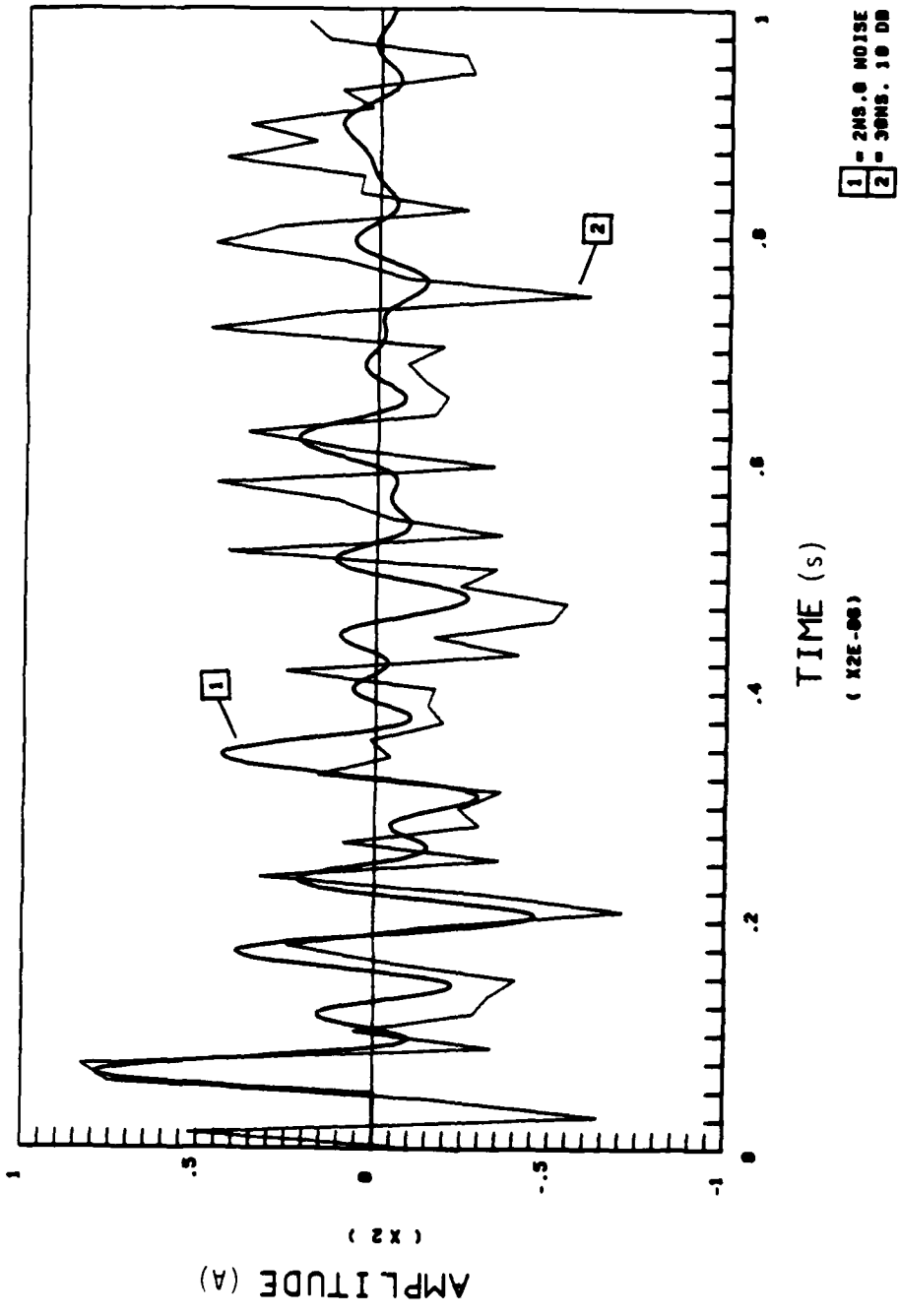

Figure 23. Large aircraft interior time domain response for 2 and 30 ns sampling intervals and 10 dB SNR.

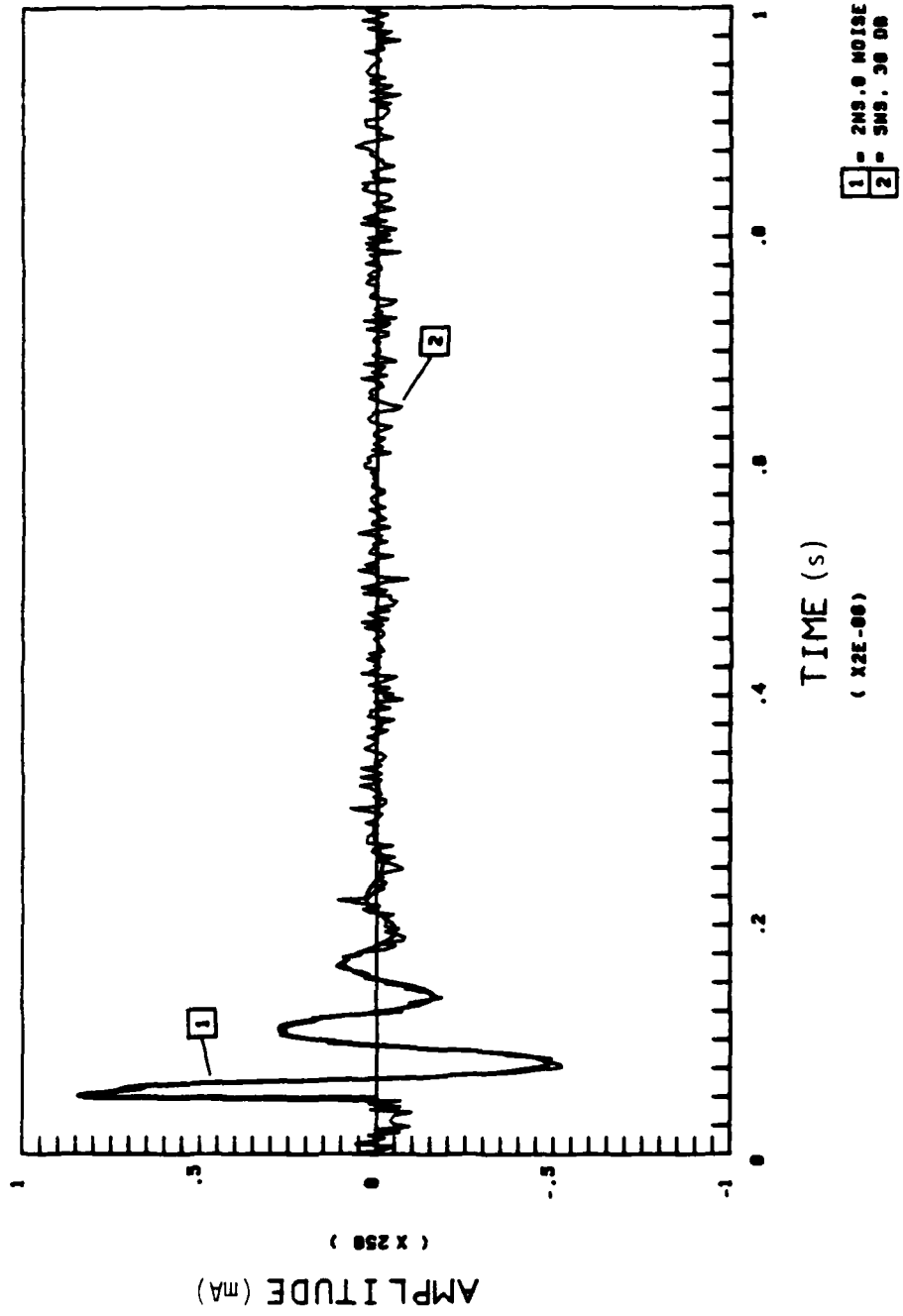

Figure 24. Small aircraft external time domain response for 2 and 5 ns sampling intervals and 30 dB SNR.

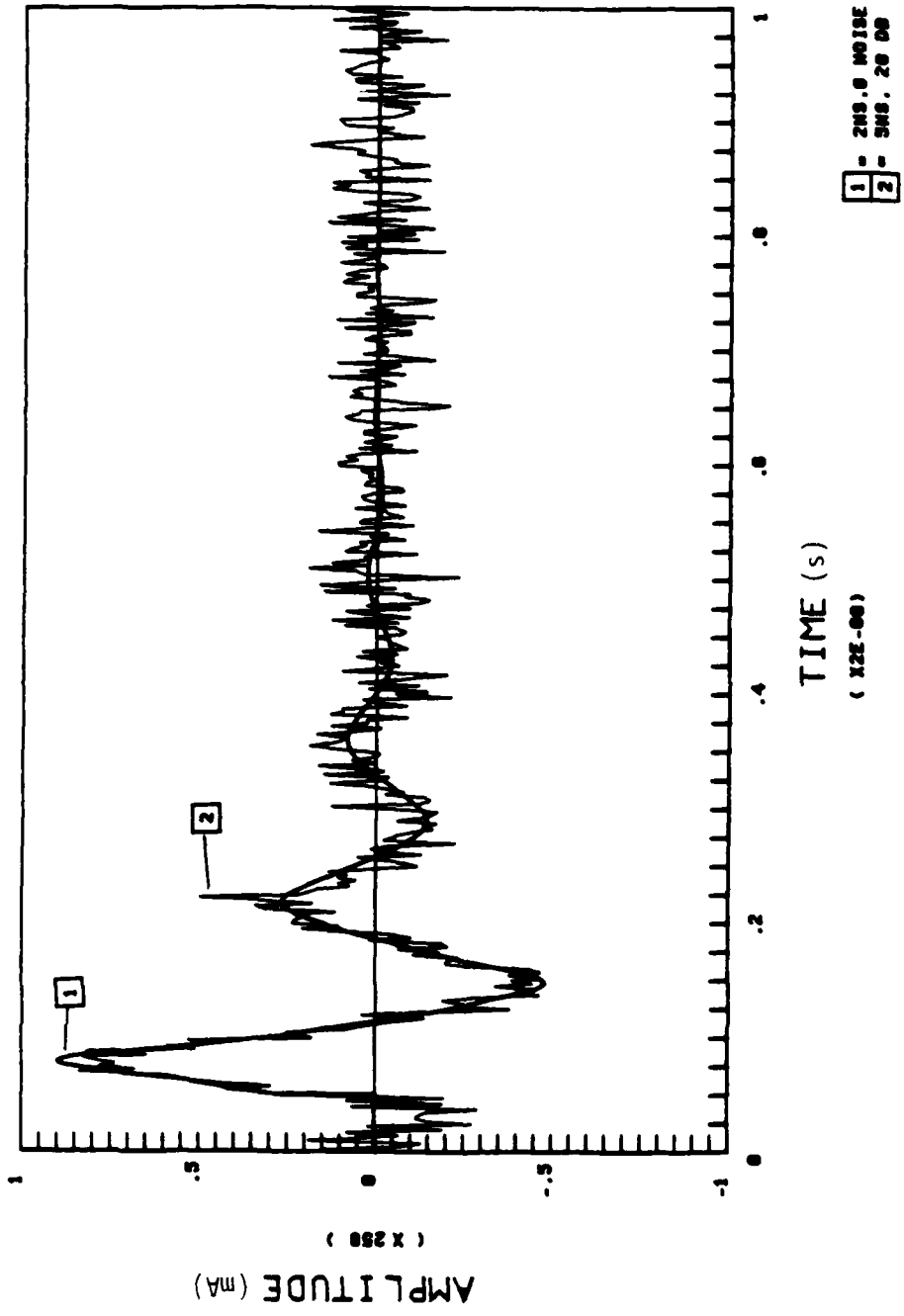

Figure 25. Large aircraft external time domain response for 2 and 5 ns sampling intervals and 20 dB SNR.

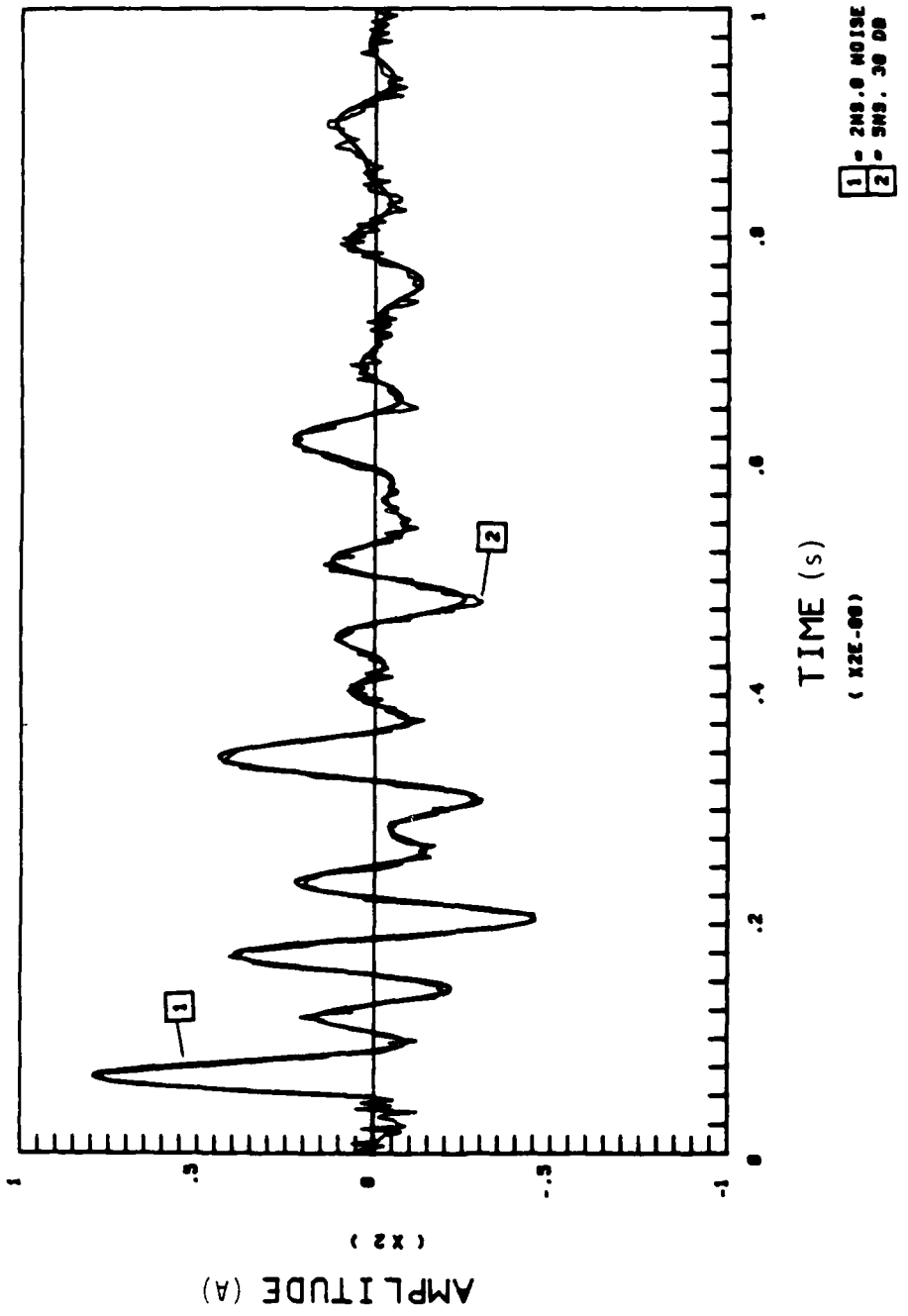

Figure 26. Large aircraft interior time domain response for 2 and 5 ns sampling intervals and 30 dB SNR.

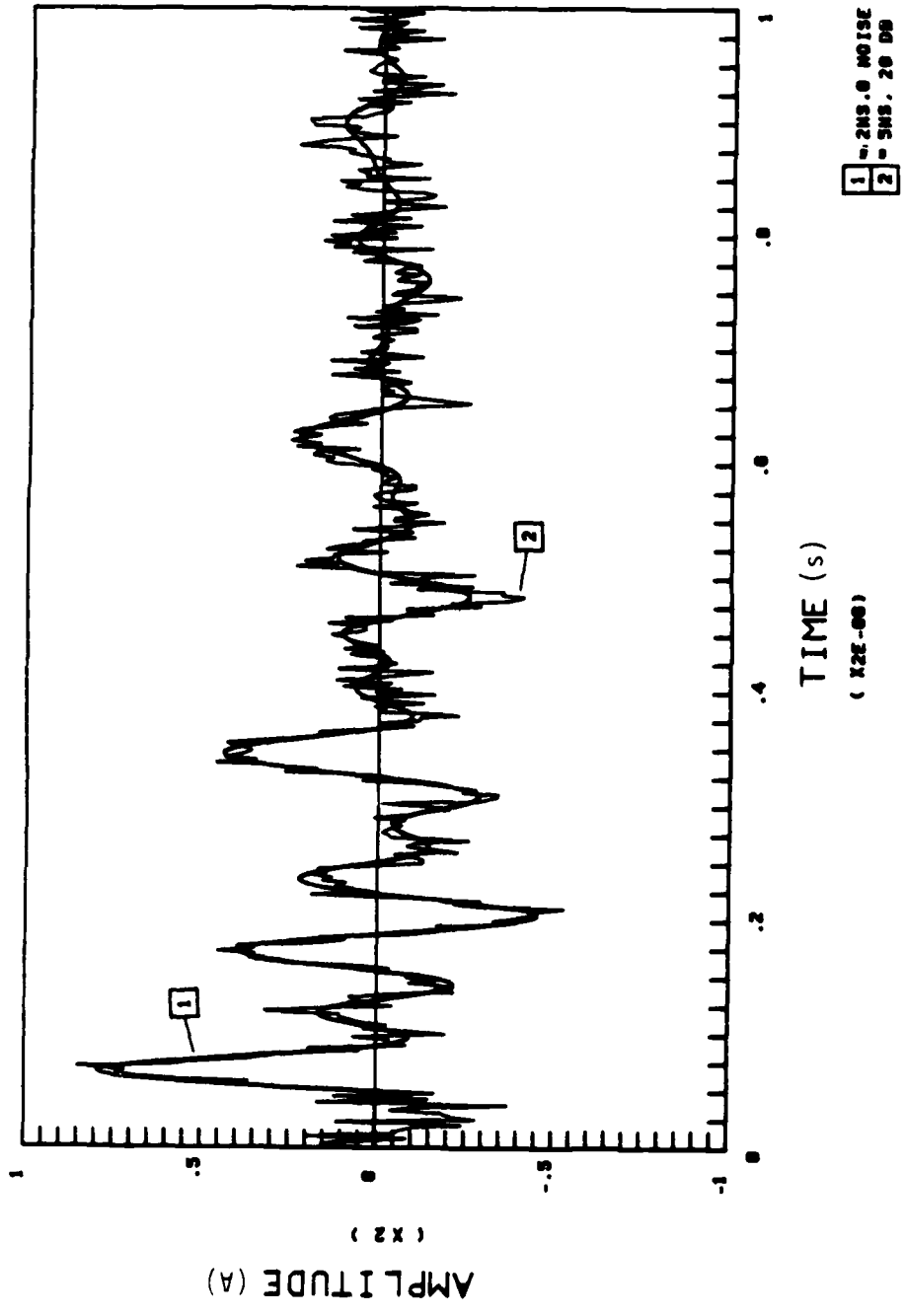

Figure 27. Large aircraft interior time domain response for 2 and 5 ns sampling intervals and 0 and 20 dB SNRs.

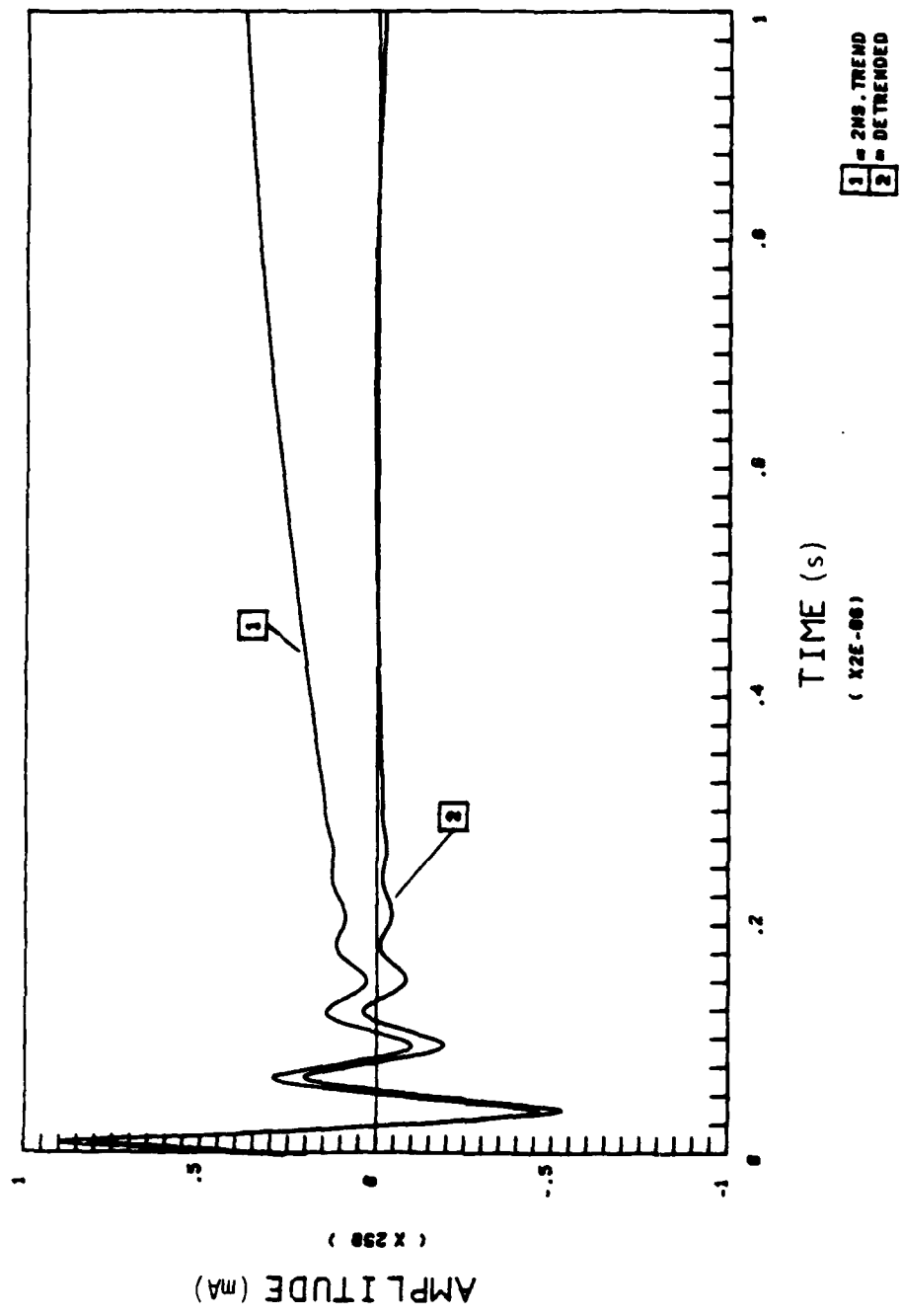

Figure 28. Small aircraft exterior time domain response for (1) 2 ns sampling interval and (2) detrended sample.

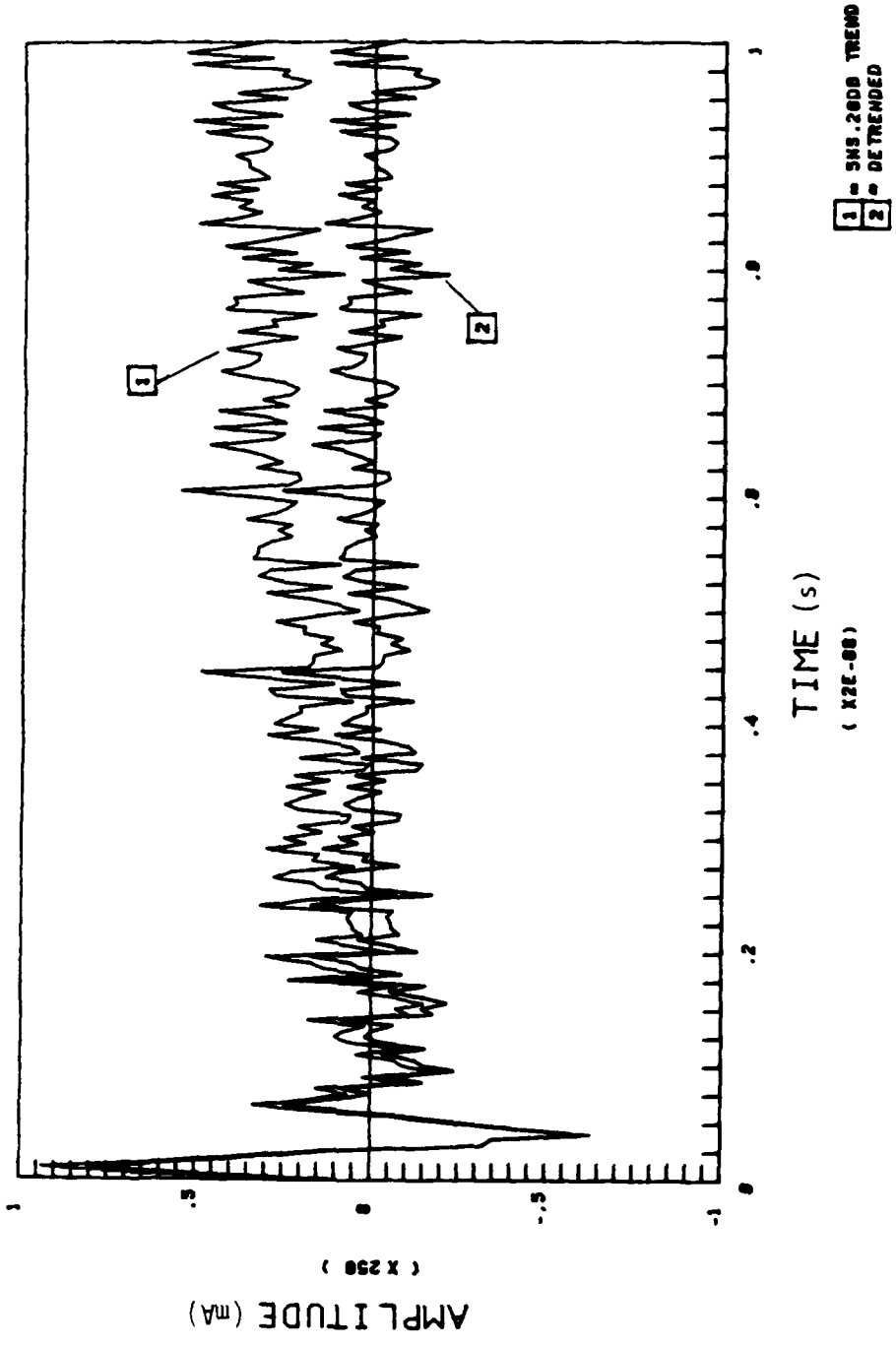

Figure 29. Small aircraft external time domain response for (1) a 5 ns sampling interval and 20 dB SNR trend and (2) detrended sample.

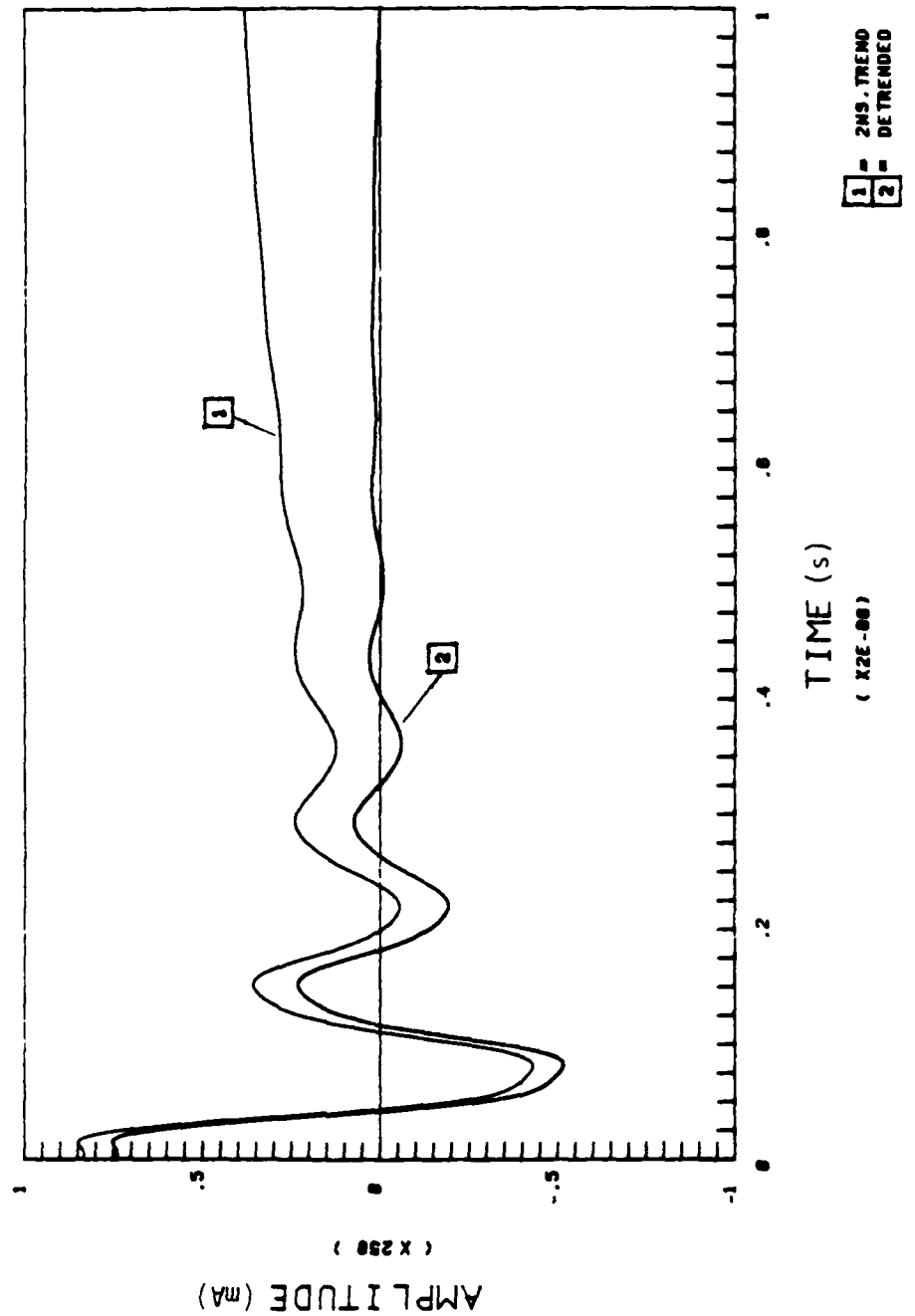

Figure 30. Large aircraft external time domain response for (1) 2 ns sampling interval trend and (2) detrended sample.

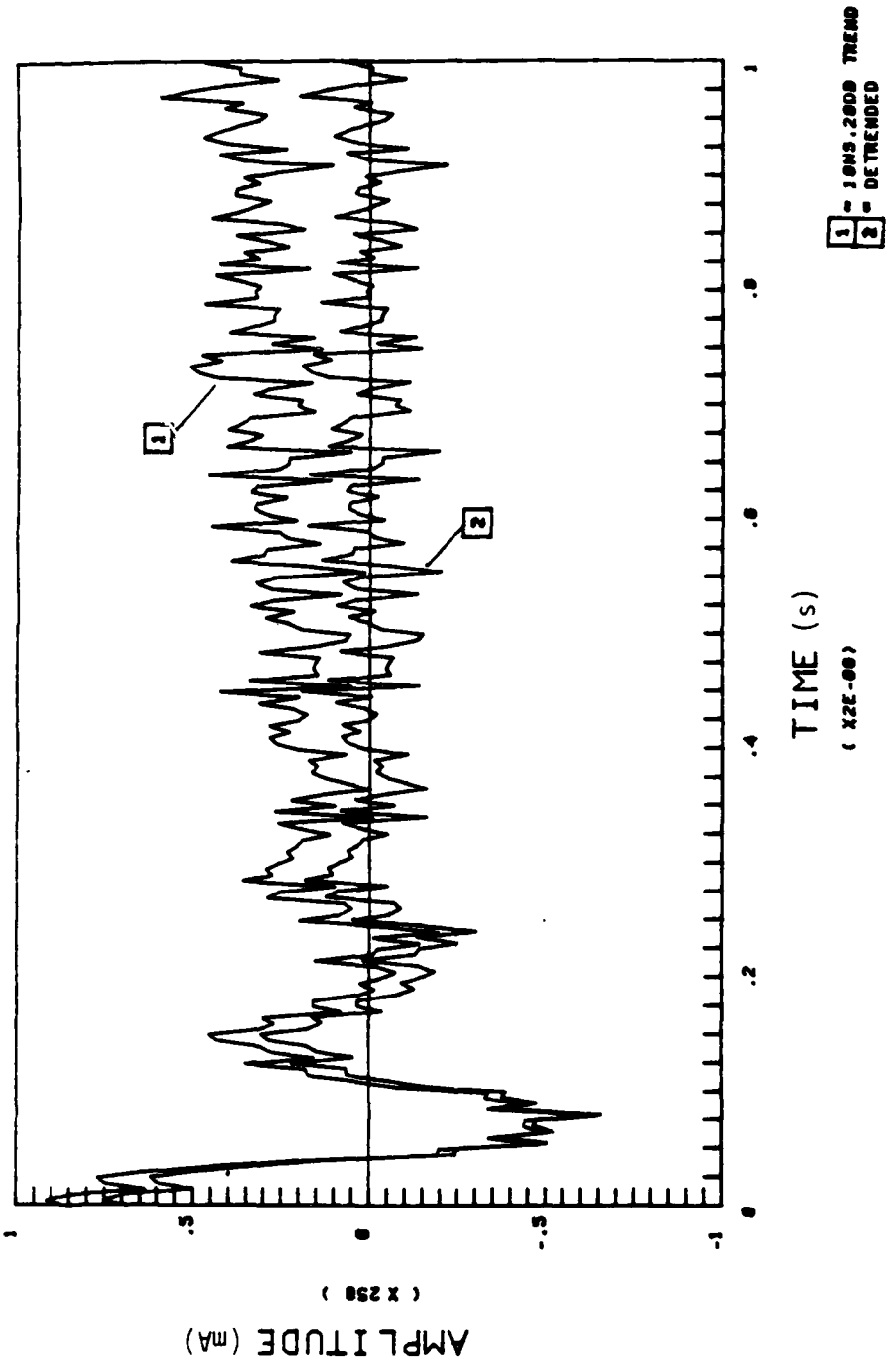

Figure 31. Large aircraft external time domain response for (1) 10 ns sampling interval and 20 dB SNR trend and (2) detrended sample.

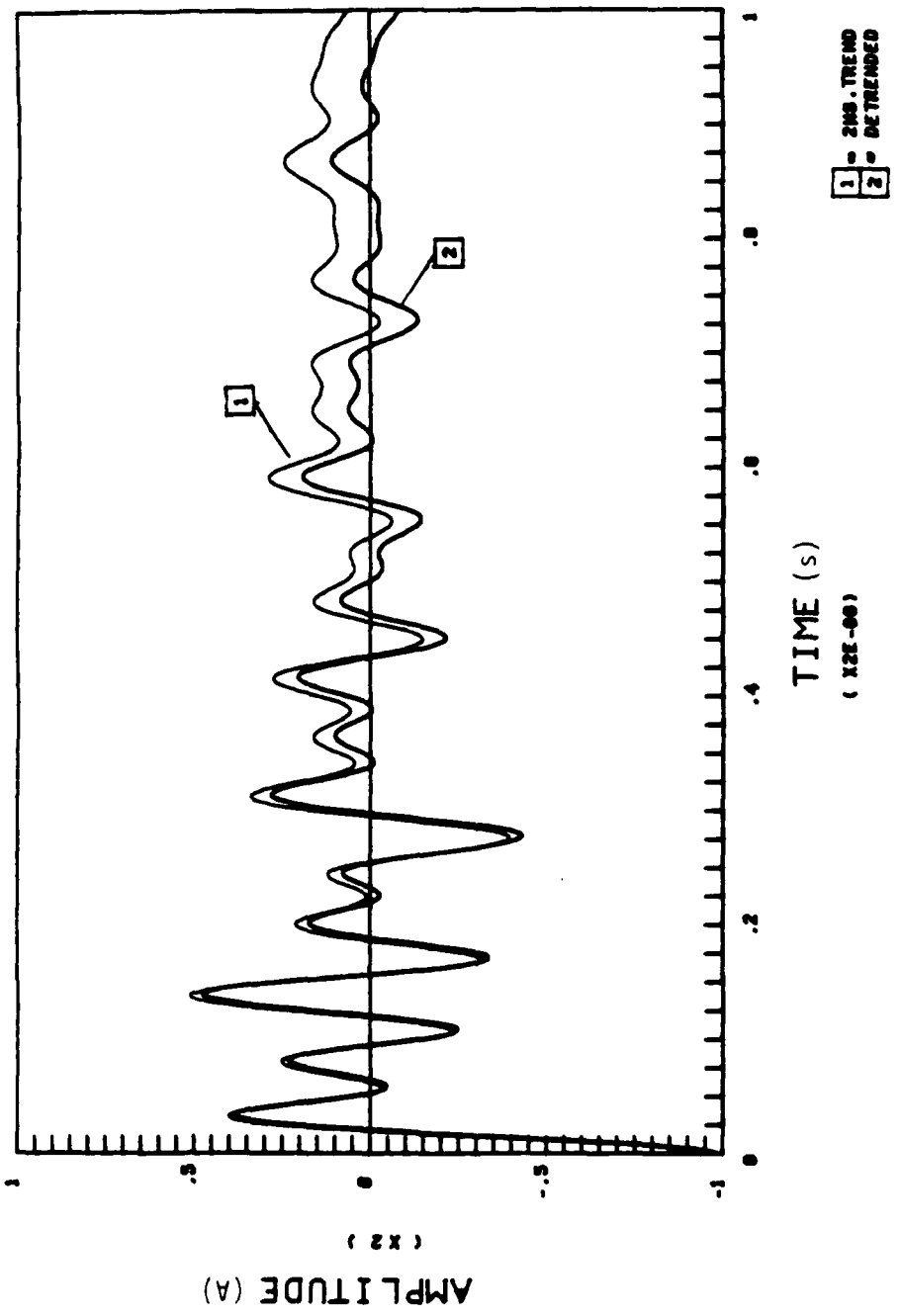

Figure 32. Large aircraft internal time domain response for (1) 2 ns sampling interval trend and (2) detrended sample.

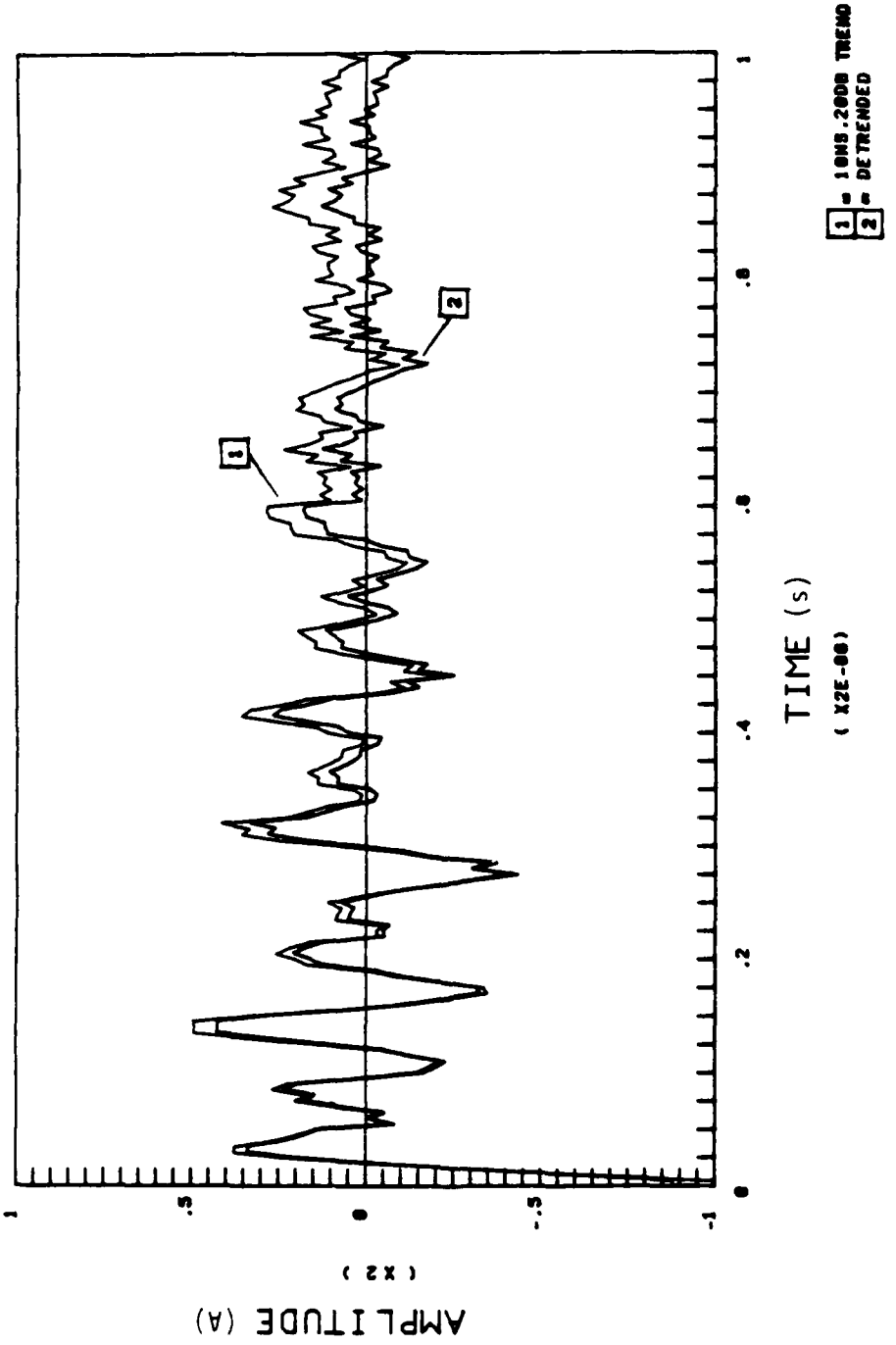

Figure 33. Large aircraft internal time domain response for (1) 10 ns sampling interval and 20 dB SNR trend and (2) detrended sample.

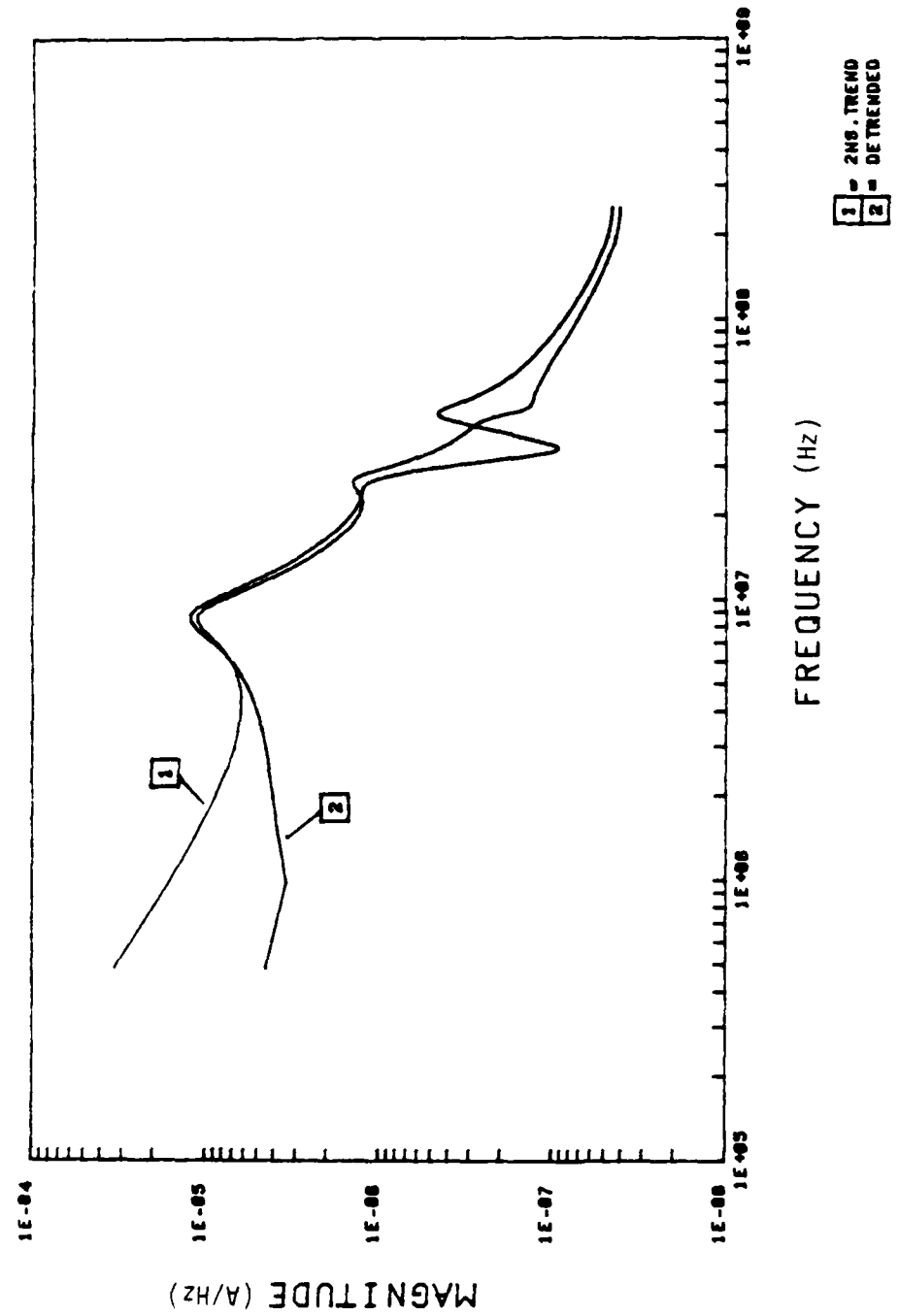

Figure 34. Small aircraft external response for (1) 2 ms sampling interval trend and (2) detrended sample.

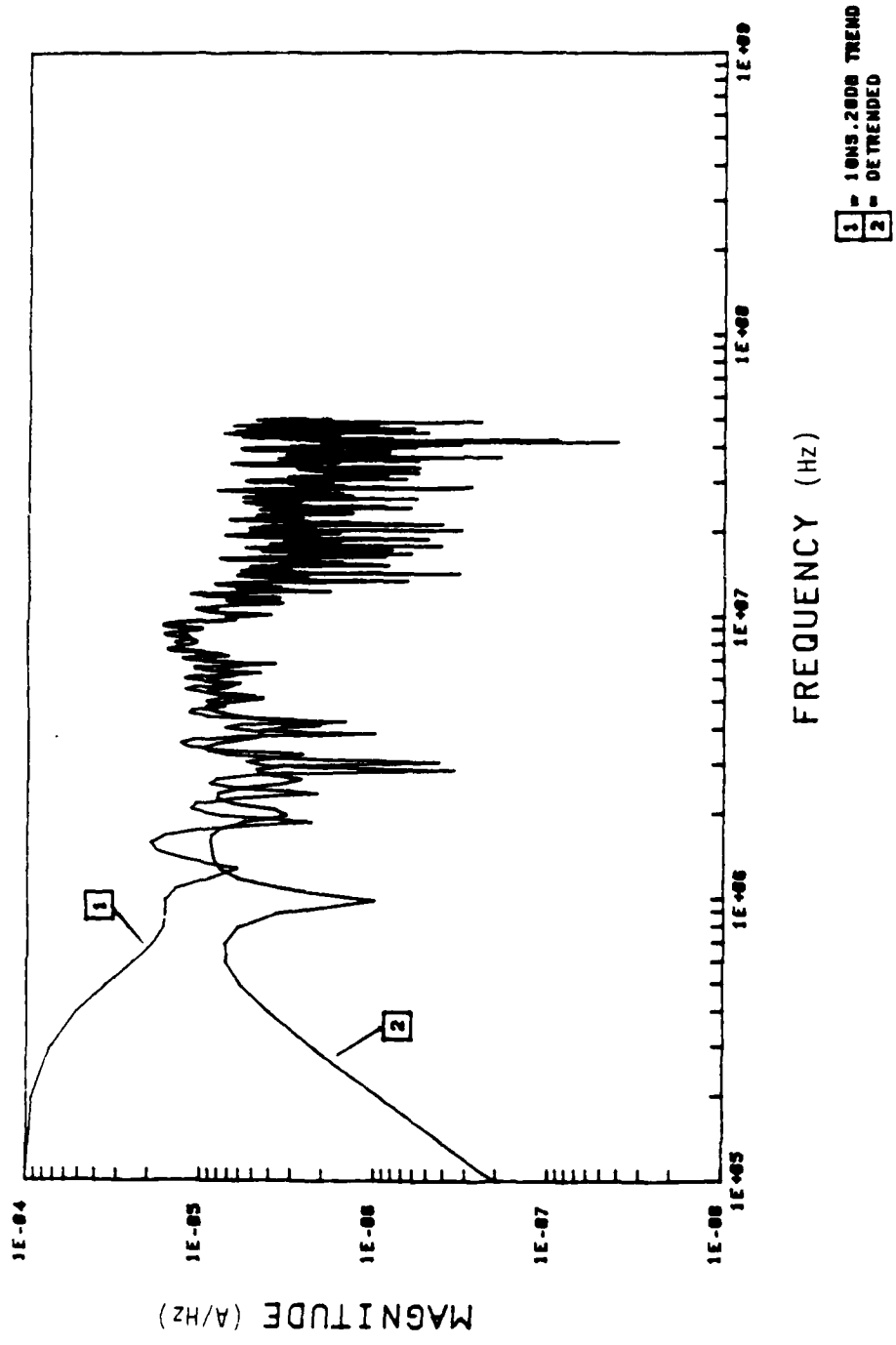

Figure 35. Small aircraft external response for (1) 10 ns sampling interval and 20 dB SNR trend and (2) detrended sample.

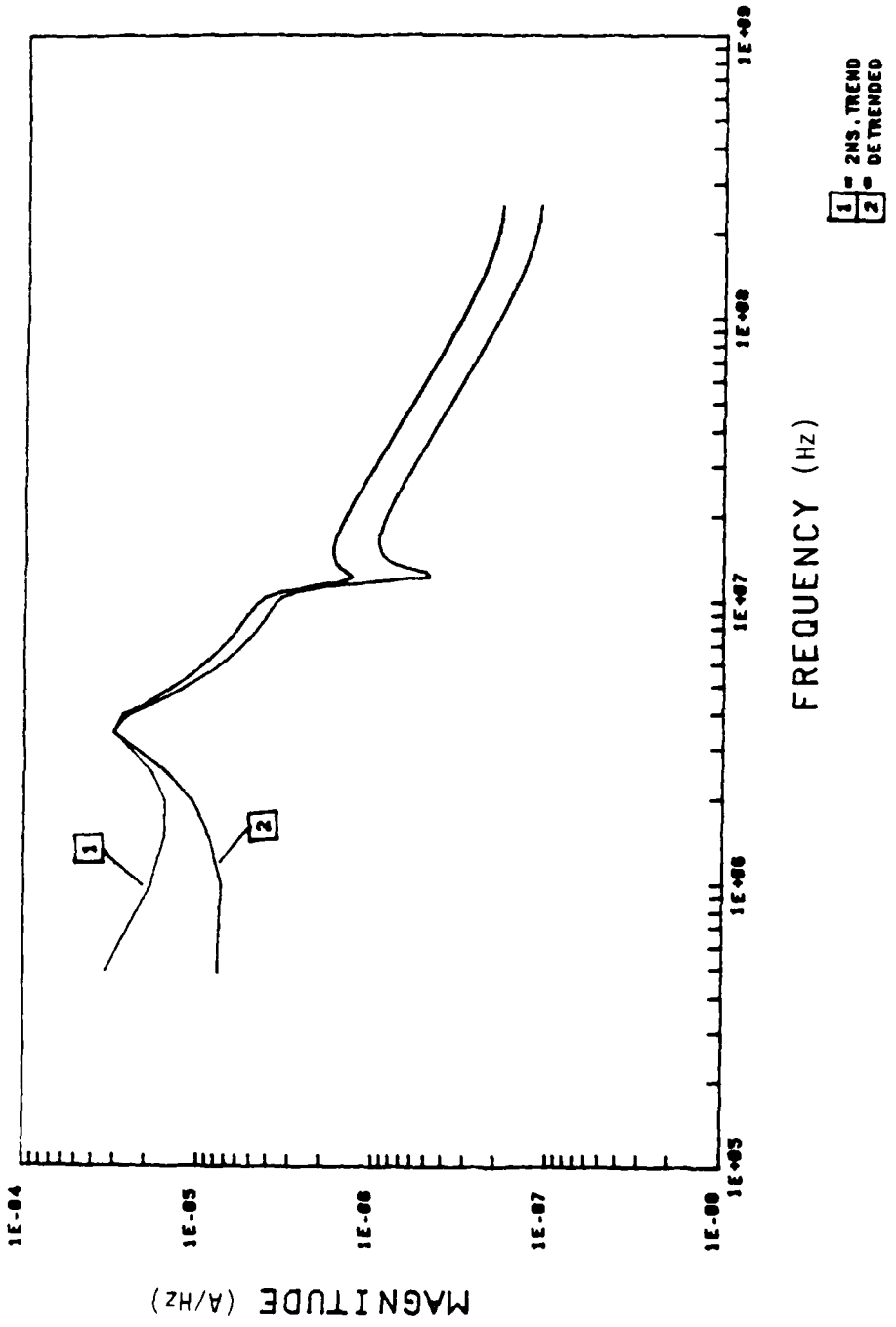

Figure 36. Large aircraft external response for (1) 2 ns sampling interval trend and (2) detrended sample.

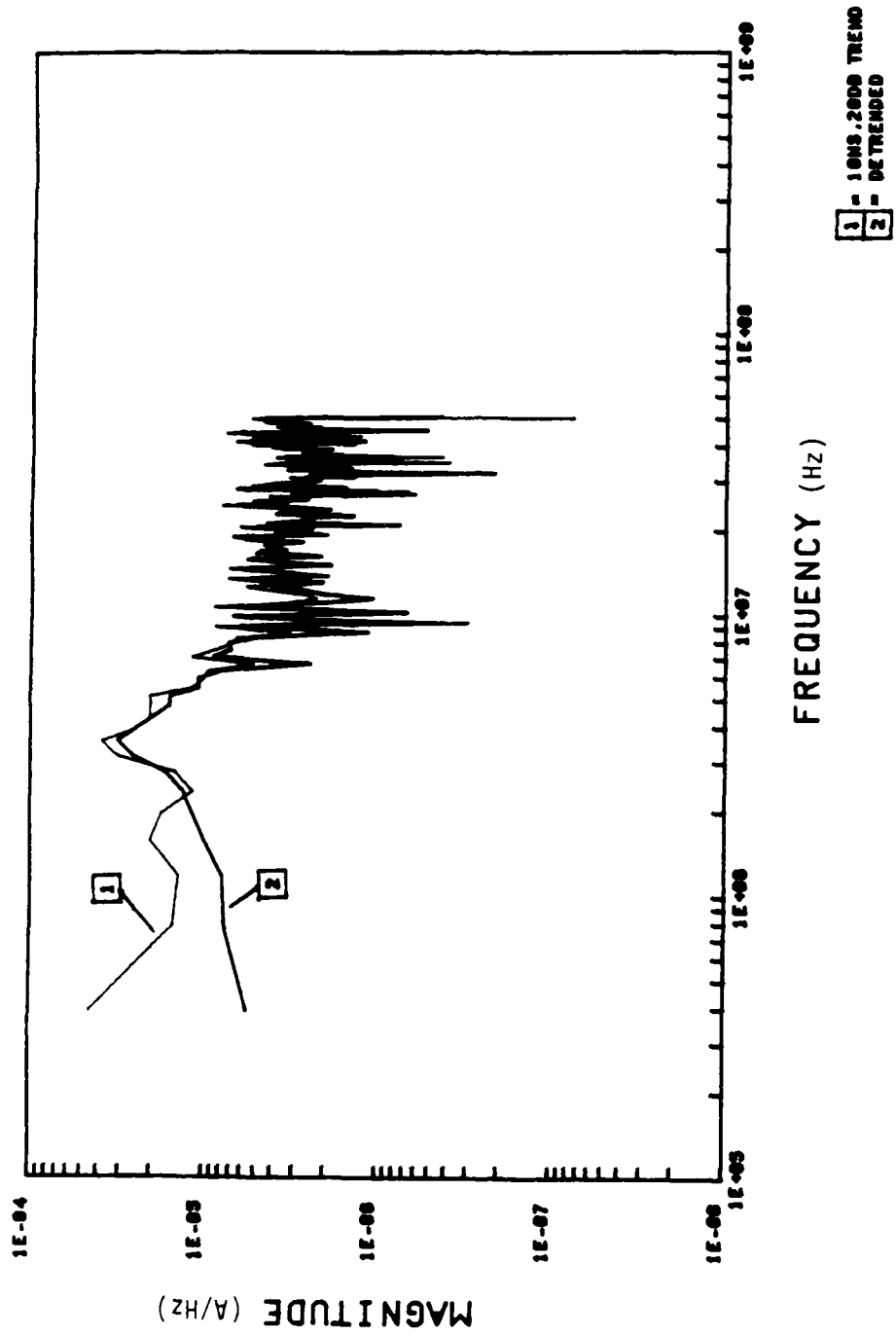

Figure 37. Large aircraft external response for (1) 10 ns sampling interval and 20 dB SNR trend and (2) detrended sample.

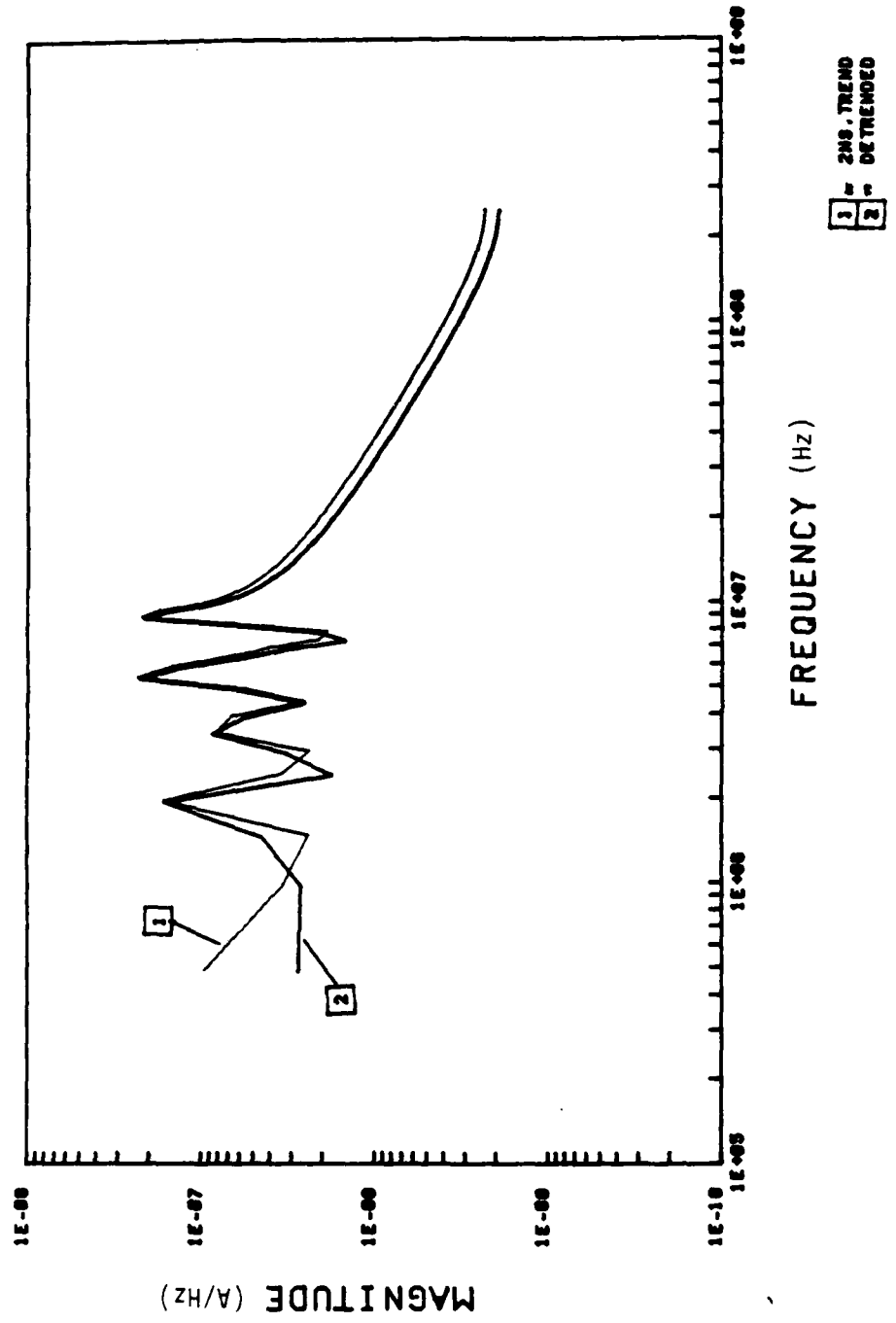

Figure 38. Large aircraft internal response for (1) 2 ns sampling interval trend and (2) detrended sample.

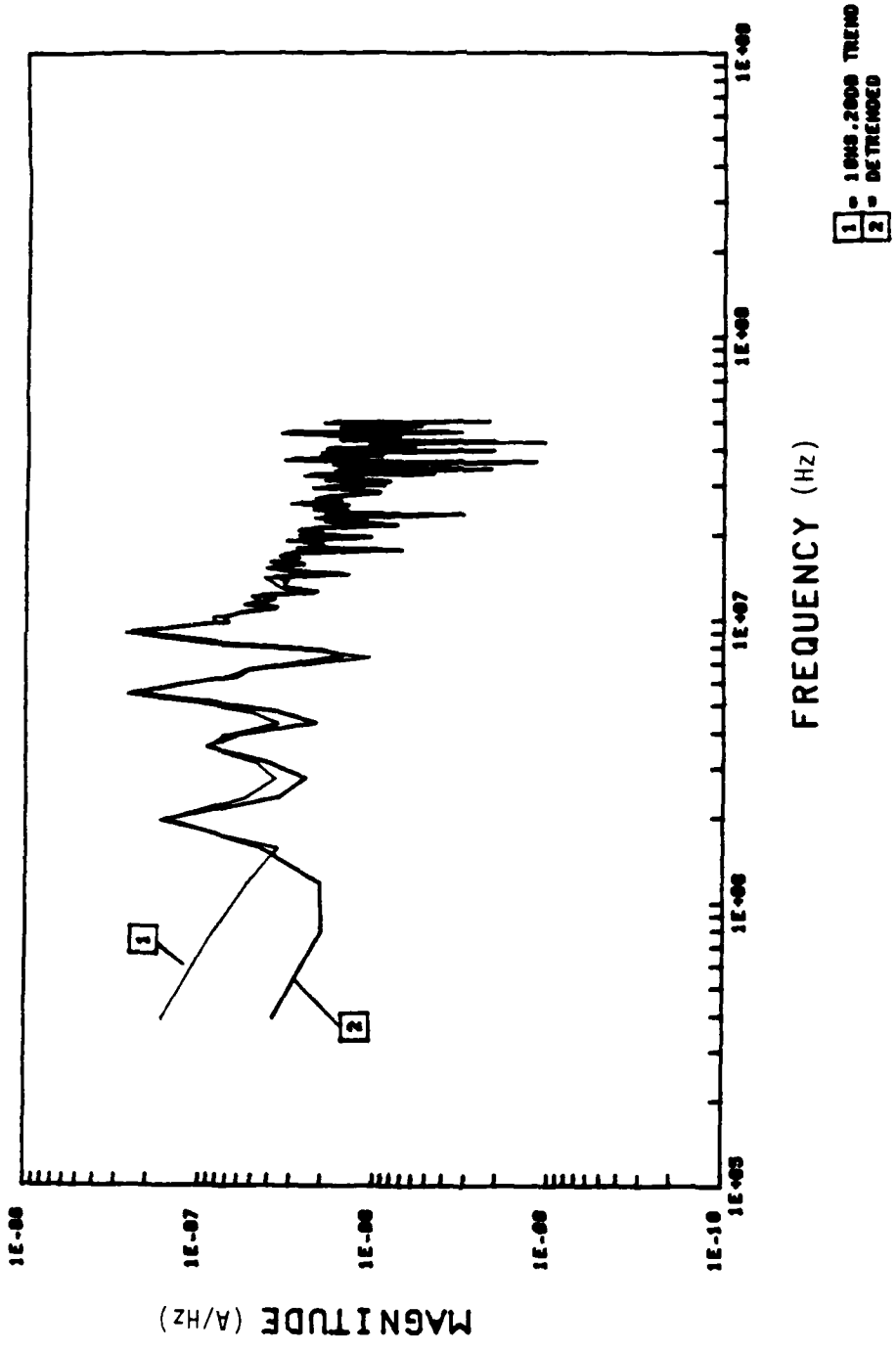

Figure 39. Large aircraft internal response for (1) 10 ns sampling interval and 20 dB SNR trend and (2) detrended sample.

REFERENCES

1. Gonzales, M., et al., Posttest Analysis for EMP Facilities/Test Operation Improvement, AFWL-TR-84-03, Air Force Weapons Laboratory, Kirtland Air Force Base, NM, June 1984.

2. Baum, C. E., "Norms of Time-Domain Functions and Convolution Operators," Mathematics Notes, Note 86, Air Force Weapons Laboratory, Kirtland Air Force Base, NM, December 1985.

3. Otnes, R. K. and Enochson, L., Applied Time Series Analysis, Vol. 1, Basic Techniques, John Wiley: New York, 1978.

4. Taylor, C. D., Giles, S., and Harper, E., "Pulse Data Preprocessing Techniques to Recover SEM Parameters," to be presented at the 1987 National Radio Science Meeting, Boulder, CO, January 1987.

5. Prather, W. D., Marin, L., and Kehrer, W. S., "Development of Aircraft EMP Standards," Nuclear EMP Meeting, University of New Mexico, Albuquerque, NM, May 19-22, 1986.

6. Balestri, R. J., "Transient Instrumentation Correction," Nuclear EMP Meeting, University of New Mexico, Albuquerque, NM, May 19-22, 1986.

7. Cake, B., Ems, S., and Lentsch, D. W., "Waveform Digitizer Shares Single-Shot Events at 1.348 G. samples/s," Electronic Design, Vol. 5, pp. 117-126, March 6, 1986.